

Table 1. Continued

Subject ID	P1	P2	P3	P4	P5	P6	P7	P8	P9	P10	P11	P12
Hip dislocation	-	-	-	+	-	+	-	-	-	+	+	+
Clubfeet	-	-	+	-	-	-	+	-	-	+	+	-
Muscular hypotonia	-	-	+	-	-	-	-	-	++	++	++	++
Skin and Hair												
Doughy skin	ND	ND	+	-	-	-	+	-	++	+	+	+
Hyperextensibility	ND	ND	+	-	-	-	+	-	++	+	+	-
Cutis laxa	ND	ND	-	-	-	-	-	-	+	+	-	+
Sparse hair	ND	ND	-	-	-	-	-	-	+	+	+	-
Others			MR, DD				camptodactyly			DD		pectus excavatum
Radiological Features												
Platyspondyly	+ ^c	+ ^c	+ ^c	+	+	+	+	+	+	+	+	+
Anterior beak of vertebral body ^b	+	+	- (4 years)	- (5 years)	+	+	+	-	+	+	+	+
Short ilia	+	+	+	+	+	+	+	+	+	+	+	+
Prominent lesser trochanter	+	+	+	-	+	+	+	+	+	+	+	+
Metaphyseal flaring	+	+	+	+	+	+	+	+	+	-	+	+
Epiphyseal dysplasia of femoral head	-	-	-	+	-	+	-	-	-	-	+	+
Elbow malalignment	ND	ND	+	+	+	+	+	+	+	+	+	+
Advanced carpal ossification ^b	- (9 years)	ND	- (12 years)	+	+	+	+	ND	+	- (7 years)	-	- (5 years)
Carpal fusion	ND	ND	+	-	-	-	-	-	-	-	-	-
Metacarpal shortening	ND	ND	+	+	+	+	+	+	-	-	+	-
Overtubulation	-	-	-	-	-	-	-	-	+	+	+	+

Abbreviations are as follows: SEMD-JL1, spondyloepimetaphyseal dysplasia with joint laxity type 1; EDS-PF, Ehlers-Danlos syndrome, progeroid form; ND, no data; MR, mitral regurgitation; DD, developmental delay.
^aAt last presentation.
^bAge at medical attention provided in parentheses.
^cAbsent at age 20 years in P1 and P2 and at age 12 years in P3.

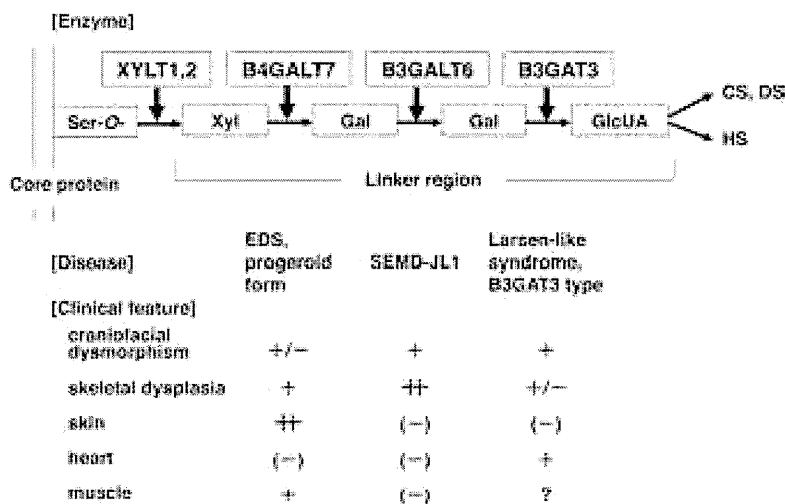


Figure 1. Enzymes Involved in Biosynthesis of the Glycosaminoglycan Linker Region and Summary Features of Diseases Caused by Their Defects Based on a Conventional Concept for the Diseases

The biosyntheses of GAGs start with the formation of a common tetrasaccharide linker sequence covalently attached to the core protein. The linker region synthesis involves a single linear pathway composed of four successive steps catalyzed by distinctive enzymes. Abbreviations are as follows: XYLT, β -xylosyltransferase; B4GALT7, xylosylprotein β 1,4-galactosyltransferase, polypeptide 7 (β 1,4-galactosyltransferase-I); B3GALT6, UDP-Gal, β Gal β 1,3-galactosyltransferase polypeptide 6 (β 1,3-galactosyltransferase-II); B3GAT3, β -1,3-glucuronyltransferase 3 (glucuronosyltransferase I); Ser-O, the serine residue of the GAG attachment site on the proteoglycan core protein; CS, chondroitin sulfate; DS, dermatan sulfate; HS, heparin sulfate.

Ehlers-Danlos syndrome; SEMD-JL1, spondyloepimetaphyseal dysplasia with joint laxity type 1.

from peripheral blood, saliva, or Epstein-Barr virus-immortalized lymphocyte of the individuals with SEMD-JL1 and/or their parents after informed consent. The study was approved by the ethical committee of RIKEN and participating institutions. We captured the exomes of the seven subjects as previously described.^{6,7} In brief, we shared genomic DNA (3 μ g) by Covaris S2 system (Covaris) and processed with a SureSelect All Exon V4 kit (Agilent Technologies). We sequenced DNAs captured by the kit with HiSeq 2000 (Illumina) with 101 base pair-end reads. We performed the image analysis and base calling by HiSeq Control Software/Real Time Analysis and CASAVA1.8.2 (Illumina) and mapped the sequences to human genome hg19 by Novoalign. We processed the aligned reads by Picard to remove PCR duplicate. The mean depth of coverage for reads was 132.8 \times , and, on average, 91.0% of targeted bases had sufficient coverage (20 \times coverage) and quality for variant calling (Table S1 available online). The variants were called by Genome Analysis Toolkit 1.5-21 (GATK) with the best practice variant detection with the GATK v.3 and annotated by ANNOVAR (2012 February 23).

Based on the hypothesis that SEMD-JL1 is inherited in an autosomal-recessive fashion, we filtered variants with the script created by BITS (Tokyo, Japan) according to following conditions: (1) variants registered in ESP5400, (2) variants found in our in-house controls (n = 274), (3) synonymous changes, (4) rare variants registered in dbSNP build 135 (MAF < 0.01), and (5) variants associated with segmental duplication. After combining variants selected by the homozygous mutation model and the compound heterozygous mutation model, we selected genes shared by individuals from three or more families. The analysis of the next-generation sequencing identified possible compound heterozygous variants in *B3GALT6* in individuals from three families (Table S2). In addition, two other subjects had possible causal heterozygous variants of *B3GALT6*.

B3GALT6 (RefSeq accession number NM_080605.3) is a single-exon gene on chromosome 1p36.33. It encodes UDP-Gal: β Gal β 1,3-galactosyltransferase polypeptide 6 (or galactosyltransferase-II: GalT-II), an enzyme involved in the biosynthesis of the glycosaminoglycan (GAG) linker region.⁸ The biosyntheses of dermatan sulfate (DS), chondroitin sulfate (CS), and heparin/heparan sulfate (HS) GAGs start with the formation of a tetrasaccharide linker sequence, glucuronic acid- β 1-3-galactose- β 1-3-galactose- β 1-4-xylose- β 1 (GlcUA-Gal-Gal-Xyl), which is covalently attached to the core protein. The linker region synthesis involves a single linear pathway composed of four successive steps catalyzed by distinctive enzymes (Figure 1). The first step is the addition of xylose to the hydroxy group of specific serine residues on the core protein by xylosyltransferases from UDP-Xyl, followed by two distinct galactosyltransferases (GalT-I and II) and a glucuronosyltransferase from UDP-Gal and UDP-GlcUA, respectively. The next hexamine addition is critical because it determines which GAG (i.e., CS, DS, or HS) is assembled on the linker region. GalT-II encoded by *B3GALT6* functions in the third step of the linker formation (Figure 1).

To confirm the results obtained by the next-generation sequencing, we examined the seven subjects used for the next-generation sequencing and an additional subject from a Vietnamese family (F7) by direct sequence of the PCR products from genomic DNAs using 3730xl DNA Analyzer (Applied Biosystems). The Sanger sequencing confirmed all *B3GALT6* mutations found by the next-generation sequencing and identified additional *B3GALT6* mutations. The results indicated that *B3GALT6* mutations were found in all subjects (Tables 2 and S1). All but P4 from F3 were compound heterozygotes of missense mutations. In P4, only a heterozygous c.1A>G (p.Met1?) mutation was found, although we searched for a *B3GALT6* mutation in the entire coding region, 5' and 3' UTRs, and flanking

Table 2. B3GALT6 Mutations in Spondyloepimetaphyseal Dysplasia with Joint Laxity Type 1 and Ehlers-Danlos Syndrome, Progeroid Form

Family	Clinical Diagnosis	Nucleotide Change	Amino Acid Change
F1	SEMD-JL1	c.1A>G	p.Met1?
		c.694C>T	p.Arg232Cys
F2	SEMD-JL1	c.1A>G	p.Met1?
		c.466G>A	p.Asp156Asn
F3 ^a	SEMD-JL1	c.1A>G	p.Met1?
F4	SEMD-JL1	c.1A>G	p.Met1?
		c.694C>T	p.Arg232Cys
F5	SEMD-JL1	c.694C>T	p.Arg232Cys
		c.899G>C	p.Cys300Ser
F6	SEMD-JL1	c.1A>G	p.Met1?
		c.193A>G	p.Ser65Gly
F7	SEMD-JL1	c.200C>T	p.Pro67Leu
		c.694C>T	p.Arg232Cys
F8	EDS-PF	c.353delA	p.Asp118Alafs*160
		c.925T>A	p.Ser309Thr
F9	EDS-PF	c.588delG	p.Arg197Alafs*81
		c.925T>A	p.Ser309Thr
F10	EDS-PF	c.16C>T	p.Arg6Trp
		c.415_423del	p.Met139Ala141del

The nucleotide changes are shown with respect to *B3GALT6* mRNA sequence. The corresponding predicted amino acid changes are numbered from the initiating methionine residue.

^aOnly a heterozygous mutation was found.

regions of *B3GALT6*. Most of the mutations are predicted to be disease causing by in silico analysis. The c.1A>G (p.Met1?) mutation was found in individuals from five of the seven families.

Although mutations affecting initiation codons have been reported to be pathogenic in several diseases,⁹ the effects of initiation codon mutations on the encoded protein are variable among the genes. We therefore investigated the effect of the c.1A>G (p.Met1?) mutation on the protein by using C-terminally FLAG-tagged *B3GALT6* with and without the mutation expressed in HeLa cells (RIKEN Cell Bank). We detected the mutant *B3GALT6* protein with a molecular weight ~4 kD lower compared with the wild-type (WT) protein (Figure 2A). These results suggest that translation initiation at the second ATG of the coding sequence, at position c.124, would become the initiation codon because of the mutation, probably resulting in an N-terminal deletion of 41 amino acids (p.Met1_Ala41del), in the same open reading frame that contains the transmembrane domain. We then examined the subcellular localization of the mutant *B3GALT6* protein by immunocytochemistry. The immunofluorescence for WT-*B3GALT6* was observed in a perinuclear region overlapping

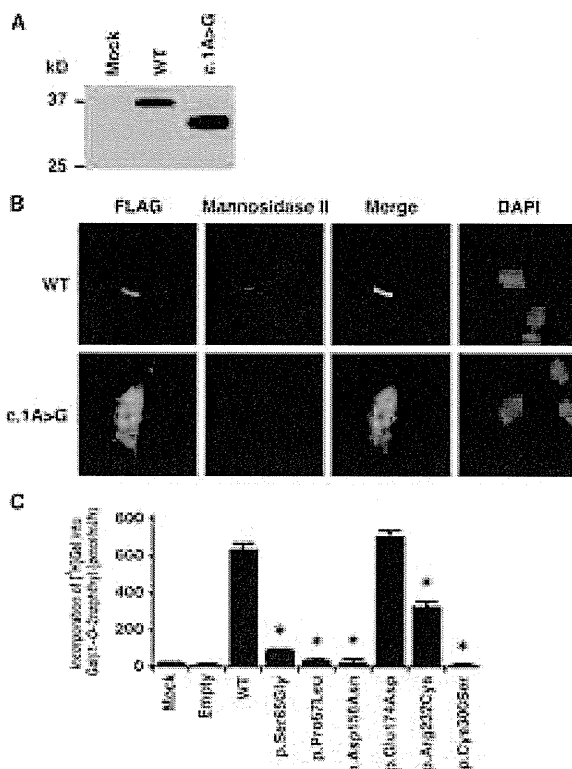


Figure 2. Analyses of *B3GALT6* Missense Mutant Proteins Identified in Individuals with SEMD-JL1 In Vitro

(A) Immunoblot analysis of lysates from HeLa cells expressing transfected wild-type (WT) and mutant (c.1A>G) *B3GALT6*. The mutant *B3GALT6* yields a shortened protein. The difference of the molecular sizes between WT and mutant proteins is approximately ~4 kD.

(B) Subcellular localization of *B3GALT6*. HeLa cells were transfected with WT and mutant (c.1A>G) *B3GALT6*. Cells were stained with anti-FLAG (green), anti- α -mannosidase II (red), and 4',6-diamidino-2-phenylindole (DAPI; blue). WT was expressed in the Golgi, but the mutant was found in cytoplasm and nucleus.

(C) Decreased enzyme activities of the missense mutant proteins (p.Ser65Gly, p.Pro67Lys, p.Asp156Asn, p.Arg232Cys, and p.Cys300Ser). p.Glu174Asp is a common polymorphism in the public database. The GalT-II activity is measured by incorporation of [³H]Gal into Gal β 1-O-2naphthyl (pmol/ml/hr) and represents the averages of three independent experiments performed in triplicate. Empty and mock indicate the GalT-II activity obtained with the conditioned medium transfected with or without an empty vector. * $p < 0.0001$ versus WT (one-way analysis of variance with Dunnett's adjustment).

with that for α -mannosidase II, a marker of the Golgi as previously reported.⁸ In contrast, the immunofluorescence for the mutant *B3GALT6* protein was observed in the nucleus and cytoplasm (Figure 2B). Therefore, the mutant protein can be considered to be functionally null because of the mislocalization.

To investigate the causality of other *B3GALT6* missense mutations, we also examined the subcellular localization of the mutant *B3GALT6* proteins by immunocytochemistry. c.193A>G (p.Ser65Gly), c.200C>T (p.Pro67Leu),

and c.694C>T (p.Arg232Cys) mutants showed mislocalization, whereas c.466G>A (p.Asp156Asn) and c.899G>C (p.Cys300Ser) mutants showed normal localization (Figure S1). To investigate whether the *B3GALT6* missense mutations affect the enzyme function, the GalT-II activities of soluble FLAG-tagged proteins for WT and mutant *B3GALT6* proteins were assayed. The GalT-II activities of p.Ser65Gly-, p.Pro67Leu-, p.Asp156Asn-, p.Arg232Cys-, and p.Cys300Ser-*B3GALT6* were significantly decreased compared with WT-*B3GALT6* (Figure 2C), indicating that these mutations resulted in a loss of enzyme function. On the other hand, there were no significant differences in the GalT-II activities between WT-*B3GALT6* and p.Glu174Asp-*B3GALT6*, a common polymorphism (rs12085009) in the public database (Figure 2C).

All SEMD-JL1 individuals with the *B3GALT6* mutation had the characteristic skeletal abnormalities, including platyspondyly, short ilia, and elbow malalignment (Table 1 and Figure S2); however, some had a range of extraskeletal and connective tissue abnormalities that overlapped with those seen in Ehlers-Danlos syndrome, progeroid form (EDS-PF [MIM 130070]). EDS-PF is an autosomal-recessive connective tissue disorder characterized by sparse hair, wrinkled skin, and defective wound healing with atrophic scars.¹⁰ In addition, skeletal abnormalities so far reported in EDS-PF are limited to generalized osteopenia and radial head dislocation, which are in contrast with the severe generalized dysplasias of the axial and appendicular skeleton observed in SEMD-JL1. Thus, both disorders at first glance appear as separate clinical entities, although they share the clinical features of short stature, joint laxity and dislocation, and facial dysmorphism. In two families with individuals with EDS-PF, recessive mutations of *B4GALT7* (MIM 604327) have been found.^{11,12} *B4GALT7* (RefSeq NM_007255.2) encodes an enzyme, xylosylated protein β -1,4-galactosyltransferase, that catalyzes the second step of the GAG linker region biosynthesis (Figure 1). Therefore, we speculated that *B3GALT6* and *B4GALT7* deficiencies might show similar phenotypes. We then examined *B3GALT6* in four additional individuals (P9–P12) who had phenotypes compatible with EDS-PF (Table 1 and Figure S3) but in whom no *B4GALT7* mutations had been found. Sanger sequencing of the EDS-PF-like subjects revealed that all were compound heterozygotes for *B3GALT6* mutations (Table 2). There were two frame-shift mutations and one missense mutation (c.925T>A [p.Ser309Thr]) common in two families (F8 and F9). We investigated the enzyme function of the missense mutation by using the same assay for SEMD-JL1 missense mutations. The GalT-II activities of p.Ser309Thr-*B3GALT6* were significantly decreased (Figure S4).

Collectively, 11 different mutations in individuals from 10 families were identified in *B3GALT6* by a combination of exome and targeted sequencing (Table 2 and Figure S5). None of these mutations were detected in more than 200 ethnicity-matched controls or in public databases, including the 1000 Genomes database, indicating that

they are unlikely to be polymorphisms. SEMD-JL1 and EDS-PF-like individuals had no common mutations (Table 2). The individuals with *B3GALT6* mutations were short at birth and their short stature worsened with age. Their common clinical features were a flat face with prominent forehead and kyphoscoliosis (Table 1). Kyphoscoliosis was noticed in infancy in most cases and even in utero in severe cases. Although skeletal changes were essentially the same, craniofacial and skin abnormalities, joint laxities, and muscular hypotonia were variable among the individuals with *B3GALT6* mutations. Common radiographic features were platyspondyly that becomes less conspicuous with age, short ilia, and elbow malalignment (Table 1). Prominent lesser trochanters and metaphyseal flaring were seen in most cases. No individuals showed generalized osteoporosis. The disease phenotype was very variable between families (mutations), but in two familial cases, phenotypes were similar between the pair of the sibs. As a corollary, our results indicate that EDS-PF is genetically heterogeneous, with a proportion of cases being caused by mutations in *B4GALT7* and another in *B3GALT6*.

Diseases caused by defects in enzymes involved in the biosynthesis of the GAG linker region are categorized as the GAG linkeropathy. The first member of GAG linkeropathy has been identified to arise from an EDS-PF/*B4GALT7* deficiency. *B4GALT7* mutations have been identified in homozygous c.808C>T (p.Arg270Cys)¹² and compound heterozygous (c.557C>A [p.Ala186Asp] and c.617T>C [p.Leu206Pro])¹¹ states. Another member of GAG linkeropathy manifests itself as Larsen-like syndrome, *B3GAT3* type (MIM 245600). A family with individuals harboring a homozygous *B3GAT3* (MIM 606374; RefSeq NM_012200.3) mutation (c.830G>A [p.Arg227Gln]) has been identified. The clinical features of five affected individuals of the family are characterized by dislocation and laxity of joints and congenital heart defects.¹¹ The former considerably overlaps with the phenotypes of SEMD-JL1 and EDS-PF, two other GAG linkeropathies; however, the association of heart defects has critically differentiated this disease from the others (Figure 1).

Given that the linker region biosynthesis is nonparallel and that the defects in the three enzymes simply affect the amounts of the linker region available to form GAGs (CS, HS, DS), phenotypic similarities of the three diseases are quite understandable. The quantitative difference of the phenotypes (severity of the diseases) most probably results from the difference in the degree of enzyme defects resulting from mutations. On the other hand, qualitative differences of the three diseases (e.g., scoliosis caused by the *B3GALT6* mutation, heart disease caused by the *B3GAT3* mutation, etc.) suggest other explanations. Tissue expression patterns of the three genes do not entirely explain the differences. We examined their mRNA expression in various human tissues, including cartilage, bone, and connective tissues by quantitative real-time PCR (Figure S6). We detected strong expression of *B3GALT6* in

Table 3. The Amount of GAGs in the Lymphoblastoid Cells from Individuals with Spondyloepimetaphyseal Dysplasia with Joint Laxity Type 1

Subject	GAG (Disaccharides/mg Acetone Powder) ^a [pmol]			
	CS/DS	CS	DS	HS
Control	62	48	29	128
SEMD-JL1				
P1	313	295	118	15
P2	345	175	60	21
P3	270	162	28	20

^aCalculated based on the peak area in chromatograms of digests with a mixture of chondroitinases ABC and AC-II (CS/DS), chondroitinases AC-I and AC-II (CS), chondroitinase B (DS), and heparinases I and III (HS).

cartilage and bone but only weak expression in skin, ligament, and tendon. *B4GALT7* expression was stronger in cartilage than *B3GALT6* and also weak in skin and ligament. *B3GAT3* expression was not specific to heart. The qualitative difference may result from the difference in the effects of the three genes on GAG formation.

To examine how *B3GALT6* mutations affects the products of GAGs in vivo, we measured the amounts of CS and HS chains at the surface of lymphoblastoid cells from the subjects by flow cytometry by using CS-stub and HS-stub antibodies as previously described.^{13–15} In brief, purified GAG fractions were treated individually with a mixture of chondroitinases ABC and AC-II, a mixture of chondroitinases AC-I (EC 4.2.2.5) (Seikagaku Corp.) and AC-II (EC 4.2.2.5) (Seikagaku Corp.), chondroitinase B (EC 4.2.2.19) (IBEX Technologies), or a mixture of heparinases-I and -III (IBEX Technologies) for analyzing the disaccharide composition of CS/DS, CS, DS, and HS, respectively. The digests were labeled with a fluorophore 2-aminobenzamide (2AB) and aliquots of the 2AB derivatives of CS/DS/HS disaccharides were analyzed by anion-exchange HPLC on a PA-03 column (YMC Co.). The HS-stub antibody (3G10) showed a markedly reduced binding to the epitopes on the subjects' cells (Figure S7). The relative numbers of the HS chains presented as the mean fluorescence intensity (MFI) of the cell population stained with the antibody for P1, P2, and P3 were 26%, 56%, and 35% of the control, respectively. On the other hand, the CS-stub antibody (2B6) showed a similar binding to the epitopes on the subjects' cells relative to those of the control (Figure S7). The MFI for P1, P2, and P3 were 114%, 104%, and 106% of the control, respectively. Furthermore, we measured disaccharide of GAG chains from lymphoblastoid cells by using anion-exchange HPLC after digestion with chondroitinase and heparinase. The amounts of the disaccharide from HS chains were significantly decreased, whereas CS and DS chains were ~5 times higher than those in the control (Table 3).

Previous biochemical studies on EDS-PF with *B4GALT7* mutations show a reduction in the synthesis of DS chains.^{16,17} The c.830G>A (p.Arg227Gln) mutation in

B3GAT3 causes a drastic reduction in GlcAT-I activity in fibroblasts of the individual with SEMD-JL1 and numbers of CS and HS chains on the core proteins at the surface of the fibroblasts are decreased to about half of the controls.¹¹ Cultured lymphoblastoid cells from individuals with a c.419C>T (p.Pro140Leu) mutation in *B3GAT3* show that defective synthesis is more pronounced for CS than for HS.¹¹ Taken together with our results, these findings suggest that the effects of the deficiencies of the three enzymes on GAG synthesis are not identical. A possible explanation for the qualitative phenotypic differences may be that the biosynthesis of the GAG linker region is not a simple step-by-step addition but involves parallel processing and/or alternative pathways. Other glycosyltransferases may have similar biochemical functions to these three enzymes and thus complement their deficient activities to variable degrees in cell- and/or tissue-specific manners, leading to differences in the amount of GAGs in the tissues. It is known that *B3GALT6* and *B4GALT7* have several homologs.¹⁸ It must be noted that all biochemical studies so far have been performed in vitro or in cultured cells, and therefore there is a severe limitation to our understanding of the pathogenesis at tissue and organ levels.

By exome sequencing, we identified loss-of-function mutations in *B3GALT6* in 12 individuals from 10 families. The mutations produced a spectrum of connective tissue disorders characterized by lax skin, muscle hypotonia, joint dislocation, and skeletal dysplasia and deformity, which include phenotypes previously known as SEMD-JL1 and EDS-PF (Figures S1 and S2). The pleiotropic phenotypes of *B3GALT6* mutations indicate that *B3GALT6* plays critical roles in development and homeostasis of various tissues, including skin, bone, cartilage, tendons, and ligaments. Biochemical studies that used lymphoblastoid cells of the individuals with *B3GALT6* mutations showed a decrease of HS and a paradoxical increase of CS and DS of the cell surface. Further clinical, genetic, and biological studies are necessary to understand the pathological mechanism of the diseases caused by enzyme defects involved in the biosynthesis of the GAG linker region and roles of the region in GAG metabolism and function.

Supplemental Data

Supplemental Data include seven figures and two tables and can be found with this article online at <http://www.cell.com/AJHG/>.

Acknowledgments

We thank the individuals with the disease and their family for their help to the study. We also thank the Japanese Skeletal Dysplasia Consortium. This study is supported by research grants from the Ministry of Health, Labor, and Welfare (23300101 to S.I. and N. Matsumoto; 23300201 to S.I.), by Grants-in-Aid for Young Scientists (23689052 to N. Miyake and 23790066 to S.M.) from the Japan Society for the Promotion of Science; by the Matching Program for Innovations in Future Drug Discovery and Medical Care

(K.S.); by The Ministry of Education, Culture, Sports, Science and Technology, Japan (MEXT); by a Grant-in-aid for Encouragement from the Akiyama Life Science Foundation (S.M.); by Swiss National Science Foundation Grants (31003A_141241 and 310030_132940); by The CoSMO-B project (Brazil and Switzerland); by the Leenaards Foundation (Switzerland); and by Research on intractable diseases, Health and Labour Sciences Research Grants, H23-Nanchi-Ippan-123 (S.I.).

Received: February 1, 2013

Revised: March 16, 2013

Accepted: April 5, 2013

Published: May 9, 2013

Web Resources

The URLs for data presented herein are as follows:

1000 Genomes, <http://browser.1000genomes.org>

ANNOVAR, <http://www.openbioinformatics.org/annovar/>

dbSNP, <http://www.ncbi.nlm.nih.gov/projects/SNP/>

GATK, <http://www.broadinstitute.org/gatk/>

MutationTaster, <http://www.mutationtaster.org/>

NHLBI Exome Sequencing Project (ESP) Exome Variant Server,

<http://evs.gs.washington.edu/EVS/>

Novoalign, <http://www.novocraft.com/main/page.php?s=novoalign>

Online Mendelian Inheritance in Man (OMIM), <http://www.omim.org/>

Picard, <http://picard.sourceforge.net/>

PolyPhen, <http://www.genetics.bwh.harvard.edu/pph2/>

RefSeq, <http://www.ncbi.nlm.nih.gov/RefSeq>

SIFT, <http://sift.bii.a-star.edu.sg/>

UCSC Genome Browser, <http://genome.ucsc.edu>

References

- Warman, M.L., Cormier-Daire, V., Hall, C., Krakow, D., Lachman, R., LeMerrer, M., Mortier, G., Mundlos, S., Nishimura, G., Rimoin, D.L., et al. (2011). Nosology and classification of genetic skeletal disorders: 2010 revision. *Am. J. Med. Genet. A.* *155A*, 943–968.
- Beighton, P., Gericke, G., Kozlowski, K., and Grobler, L. (1984). The manifestations and natural history of spondylo-epimetaphyseal dysplasia with joint laxity. *Clin. Genet.* *26*, 308–317.
- Nishimura, G., Satoh, M., Aihara, T., Aida, N., Yamamoto, T., and Ozono, K. (1998). A distinct subtype of “metatropic dysplasia variant” characterised by advanced carpal skeletal age and subluxation of the radial heads. *Pediatr. Radiol.* *28*, 120–125.
- Boyden, E.D., Campos-Xavier, A.B., Kalamajski, S., Cameron, T.L., Suarez, P., Tanackovic, G., Andria, G., Ballhausen, D., Briggs, M.D., Hartley, C., et al. (2011). Recurrent dominant mutations affecting two adjacent residues in the motor domain of the monomeric kinesin KIF22 result in skeletal dysplasia and joint laxity. *Am. J. Hum. Genet.* *89*, 767–772.
- Min, B.J., Kim, N., Chung, T., Kim, O.H., Nishimura, G., Chung, C.Y., Song, H.R., Kim, H.W., Lee, H.R., Kim, J., et al. (2011). Whole-exome sequencing identifies mutations of KIF22 in spondyloepimetaphyseal dysplasia with joint laxity, leptodactylic type. *Am. J. Hum. Genet.* *89*, 760–766.
- Miyake, N., Elcioglu, N.H., Iida, A., Isguven, P., Dai, J., Murakami, N., Takamura, K., Cho, T.J., Kim, O.H., Hasegawa, T., et al. (2012). PAPSS2 mutations cause autosomal recessive brachyolmia. *J. Med. Genet.* *49*, 533–538.
- Tsurusaki, Y., Okamoto, N., Ohashi, H., Kosho, T., Imai, Y., Hibi-Ko, Y., Kaname, T., Naritomi, K., Kawame, H., Wakui, K., et al. (2012). Mutations affecting components of the SWI/SNF complex cause Coffin-Siris syndrome. *Nat. Genet.* *44*, 376–378.
- Bai, X., Zhou, D., Brown, J.R., Crawford, B.E., Hennet, T., and Esko, J.D. (2001). Biosynthesis of the linkage region of glycosaminoglycans: cloning and activity of galactosyltransferase II, the sixth member of the beta 1,3-galactosyltransferase family (beta 3GalT6). *J. Biol. Chem.* *276*, 48189–48195.
- Saunders, C.J., Minassian, B.E., Chow, E.W., Zhao, W., and Vincent, J.B. (2009). Novel exon 1 mutations in MECP2 implicate isoform MeCP2_e1 in classical Rett syndrome. *Am. J. Med. Genet. A.* *149A*, 1019–1023.
- Kresse, H., Rosthøj, S., Quentin, E., Hollmann, J., Glössl, J., Okada, S., and Tønnesen, T. (1987). Glycosaminoglycan-free small proteoglycan core protein is secreted by fibroblasts from a patient with a syndrome resembling progeroid. *Am. J. Hum. Genet.* *41*, 436–453.
- Baasanjav, S., Al-Gazali, L., Hashiguchi, T., Mizumoto, S., Fischer, B., Horn, D., Seelow, D., Ali, B.R., Aziz, S.A., Langer, R., et al. (2011). Faulty initiation of proteoglycan synthesis causes cardiac and joint defects. *Am. J. Hum. Genet.* *89*, 15–27.
- Faiyaz-Ul-Haque, M., Zaidi, S.H., Al-Ali, M., Al-Mureikhi, M.S., Kennedy, S., Al-Thani, G., Tsui, L.C., and Teebi, A.S. (2004). A novel missense mutation in the galactosyltransferase-I (B4GALT7) gene in a family exhibiting facioskeletal anomalies and Ehlers-Danlos syndrome resembling the progeroid type. *Am. J. Med. Genet. A.* *128A*, 39–45.
- Kinoshita, A., and Sugahara, K. (1999). Microanalysis of glycosaminoglycan-derived oligosaccharides labeled with a fluorophore 2-aminobenzamide by high-performance liquid chromatography: application to disaccharide composition analysis and exosequencing of oligosaccharides. *Anal. Biochem.* *269*, 367–378.
- Miyake, N., Kosho, T., Mizumoto, S., Furuichi, T., Hatamochi, A., Nagashima, Y., Arai, E., Takahashi, K., Kawamura, R., Wakui, K., et al. (2010). Loss-of-function mutations of CHST14 in a new type of Ehlers-Danlos syndrome. *Hum. Mutat.* *31*, 966–974.
- Mizumoto, S., and Sugahara, K. (2012). Glycosaminoglycan chain analysis and characterization (Glycosylation/Epimerization). In *Methods in Molecular Biology. In Proteoglycans: Methods and Protocols*, F. Rédini, ed. (New York, USA: Humana Press, Springer), pp. 99–115.
- Okajima, T., Fukumoto, S., Furukawa, K., and Urano, T. (1999). Molecular basis for the progeroid variant of Ehlers-Danlos syndrome. Identification and characterization of two mutations in galactosyltransferase I gene. *J. Biol. Chem.* *274*, 28841–28844.
- Quentin, E., Gladen, A., Rodén, L., and Kresse, H. (1990). A genetic defect in the biosynthesis of dermatan sulfate proteoglycan: galactosyltransferase I deficiency in fibroblasts from a patient with a progeroid syndrome. *Proc. Natl. Acad. Sci. USA* *87*, 1342–1346.
- Togayachi, A., Sato, T., and Narimatsu, H. (2006). Comprehensive enzymatic characterization of glycosyltransferases with a beta3GT or beta4GT motif. *Methods Enzymol.* *416*, 91–102.

Case Report

Sigmoid Colon Perforation Induced by the Vascular Type of Ehlers–Danlos Syndrome: Report of a Case

HIROSHI OMORI¹, ATSUSHI HATAMOCHI², MAKOTO KOIKE¹, YOSHITOSHI SATO¹, TOMOKI KOSHO³, YASUHIITO KITAKADO¹, TAKAFUMI OE¹, TOSHIKI MUKAI¹, YOKO HARI¹, YOSHIFUMI TAKAHASHI¹, and KENJI TAKUBO¹

¹Department of Digestive Surgery, Matsue Red Cross Hospital, 200 Horomachi, Matsue, Shimane 693-8501, Japan

²Department of Dermatology, Dokkyo Medical University, Mibu, Tochigi, Japan

³Department of Medical Genetics, Shinshu University, Matsumoto, Nagano, Japan

Abstract

The vascular type of Ehlers–Danlos syndrome (vEDS) is a rare inherited disease of the connective tissues, and is caused by abnormal type III collagen resulting from heterogeneous mutations of the type III collagen *COL3A1* gene. We herein report the case of a vEDS patient who developed a sigmoid colon perforation and was given a definitive diagnosis by a genetic and biomolecular assay. The patient demonstrated clinical manifestations caused by tissue weakness such as frequent pneumothorax events and a detached retina. During the operation, we noticed easy bruising and thin skin with visible veins on the patient's abdominal wall. Finally, a diagnosis was confirmed by the reduction of type III collagen synthesis and by the identification of a mutation in the gene for type III collagen. We conclude that it is difficult to diagnose a vEDS patient without clinical experiences and specialized genetic methods. Furthermore, all organs must be treated gently during therapy, because the tissues of vEDS patients are extremely fragile.

Key words Ehlers–Danlos syndrome · Vascular type · Perforation · Type III collagen · *COL3A1*

Introduction

The vascular type of Ehlers–Danlos syndrome (vEDS, Ehlers–Danlos syndrome type IV) is a rare, autosomal dominant disease of the connective tissues caused by abnormal type III collagen resulting from heterogeneous mutations of the type III collagen *COL3A1*

gene.^{1–4} vEDS is characterized by four clinical criteria: easy bruising, thin skin with visible veins, characteristic facial features, and the rupturing of arteries and organs.^{1–4} In addition, classic EDS patients exhibit hypermobility of the large joints and hyperextensibility of the skin.^{1,2} Typically, Ehlers–Danlos syndrome (EDS) is divided into six types, and vEDS patients follow a particularly poor clinical course caused by complications from tissue weakness.^{1,2} Twenty-five percent of vEDS patients develop one or more complications associated with tissue weakness by 20 years of age, and 80% develop some complications by 40 years. Pepin et al. reported that the calculated median survival time of vEDS patients was 48 years of age.¹ We herein present a case report of a vEDS patient who was clinically and genetically diagnosed following a sigmoid colon perforation, and review the pertinent literature.

Case Report

A 20-year-old male patient was admitted to our hospital with severe abdominal pain. The patient's abdominal wall was very hard, and muscular guarding was palpated. Enhanced computed tomography was performed immediately, and revealed free air and stool containing barium in the abdominal cavity, because the patient's colon had been examined 2 days prior for causal ascites and abdominal pain by a barium enema (Fig. 1A,B). As soon as we diagnosed the patient with generalized peritonitis due to colon perforation, an emergency operation was performed. During the operation, the patient's abdominal skin was observed to be markedly thin, with visible veins. After we decided that the sigmoid colon perforation was the cause of the generalized peritonitis, the lesion was removed and Hartmann's procedure was performed. In addition, it was revealed that the patient suffered from frequent spontaneous pneumothorax events in the past, and that his creatine kinase levels

Reprint requests to: H. Omori

Received: November 15, 2009 / Accepted: February 22, 2010

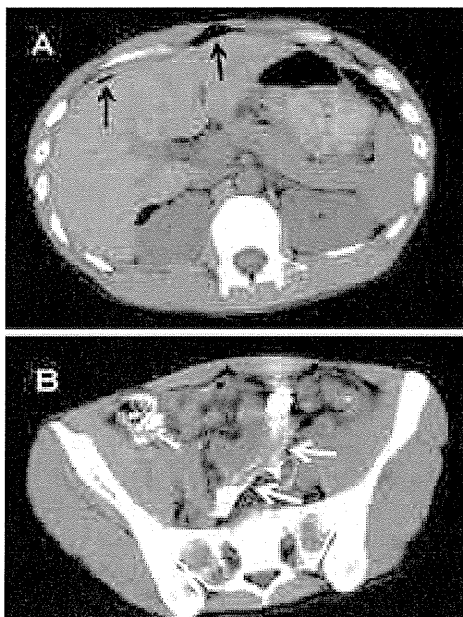


Fig. 1A,B. Enhanced computed tomography at the sigmoid colon perforation. Free air (*black arrows*) and stool containing barium (*white arrows*) were observed in the abdominal cavity

were increased to severalfold higher than in normal subjects. Although a paralytic ileus developed as a complication, the patient was discharged from our hospital 1 month after the operation. However, 3 days after discharge, he was readmitted due to his eighth spontaneous pneumothorax and a detached retina in his left eye. Because many complications caused by tissue weakness had developed over such a short period, very rare vEDS was diagnosed according to the four clinical criteria: easy bruising, thin skin with visible veins, characteristic facial features, and rupture of the arteries and organs.

To confirm this diagnosis, the patient's skin and blood samples were sent to Dokkyo Medical University, and were examined by genetic and molecular biological assays. Accordingly, the diagnosis of vEDS was confirmed by the reduction of type III collagen synthesis in cultured skin fibroblasts and by the identification of a mutation in the gene for type III collagen (*COL3A1*). The synthesis of type I collagen in this patient was the same as in controls. However, the synthesis of type III collagen was reduced by approximately 22.7% compared with normal controls (Fig. 2). A skip in exon 24 of *COL3A1*, which codes for collagen type III, was identified by genetic analysis of the complementary DNA from cultured fibroblasts (Fig. 3). Furthermore, the region near the genomic DNA was amplified by polymerase chain reaction (PCR) for the analyses of genomic DNA; the result revealed a G-to-A transition at the

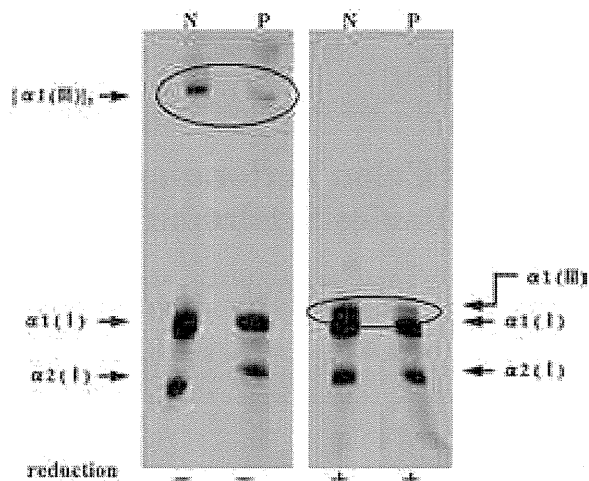


Fig. 2. Production of type I or type III collagen in the patient's cultured fibroblasts. The synthesis of type I collagen in this patient was the same as in controls. However, the synthesis of type III collagen was reduced by approximately 22.7% compared with the normal control values (*inside circle*). *N*, normal control; *P*, patient with vascular type of Ehlers-Danlos syndrome

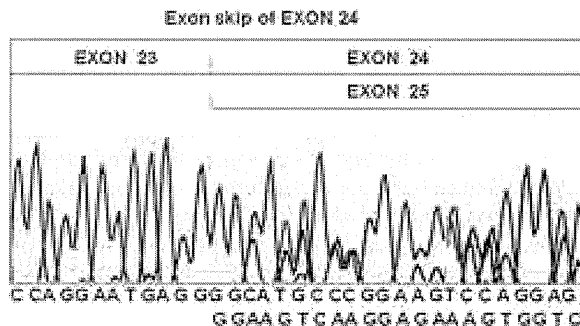


Fig. 3. Genetic analysis of the complementary DNA from the patient's cultured fibroblasts. A skip in exon 24 of *COL3A1*, which encodes collagen type III, was identified by the genetic analyses of the complementary DNA from the cultured fibroblasts

donor splice-site +1 of intron 24 (IVS 24 G+1 to A) of the *COL3A1* gene (Fig. 4). Because the mother of the present patient also demonstrated characteristic facial features and easy bruising of the skin, we genetically examined her blood samples to determine the genetic background of this patient. Consequently, we were able to confirm that the mother had the same mutation in *COL3A1* gene.

Less than 6 months after the sigmoid colon perforation, the patient was admitted with a developing

G to A transition at the donor splice-site +1 of intron 24

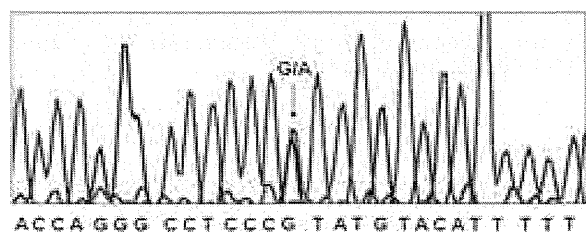


Fig. 4. Sequence analysis of genomic DNA from the patient's blood cells. The region near the genomic DNA was amplified by polymerase chain reaction for the analysis of genomic DNA. The results revealed a G-to-A transition at the donor splice site +1 of intron 24 (IVS 24 G+1 to A) of the *COL3A1* gene

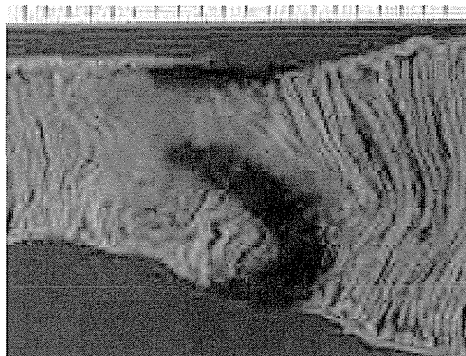


Fig. 5. Resected specimen of the jejunum from the second operation. The seromuscular layer of the patient's jejunum was torn throughout, and the entire layer of the intestine had become partly necrotic

adhesive ileus. Although conservative therapy was appropriated because there was no ischemic change of the intestine at admission, an emergency operation was performed because of the sudden onset of severe abdominal pain, which was not relieved by analgesic drugs. The operative and histopathological findings revealed the seromuscular layer of his jejunum to be torn, thus resulting in partial necrosis of this entire layer of the patient's intestine (Fig. 5). Therefore, we performed a partial resection of the small intestine, and the colostomy was not closed.

Methods of Genetic Examination

Dermal fibroblasts were obtained from the patient's skin and were cultured.⁵⁻⁷ The protein synthesis of type I and type III collagen were assessed as described previously.⁵⁻⁸ After RNA was extracted from the cultured

fibroblasts, complementary DNA was synthesized by reverse transcription from the RNA as a template. The complementary DNA was amplified by PCR, and analyzed by electrophoresis on polyacrylamide gels to identify the abnormal fragments. Abnormal DNA fragments were directly sequenced by an ABI PRISM 3100 genetic analyzer (ABI Advanced Biotechnologies, Columbia, MD, USA).^{2,3,8} Furthermore, genomic DNA was extracted from the blood cells, and all mutations were confirmed in the genomic DNA of *COL3A1* by a sequence analyzer.^{2,5,8}

Discussion

Ehlers-Danlos syndrome (EDS) is a rare inherited disease of the connective tissue.^{1,2} Most surgeons generally consider EDS to be a dermatologic disease.¹⁻⁴ However, patients who are affected by EDS, particularly the vascular EDS type (vEDS), develop complications associated with tissue weakness, and surgical or interventional therapy is often required.^{1-4,9-11} Until genetic and biochemical testing was sufficiently developed, a considerable number of patients who died unexpectedly could not be diagnosed as having vEDS. In the present case, the reason for the colonic perforation was unclear after a histopathological examination, and 6 months passed until the diagnosis of vEDS could be made by genetic and biomolecular assays. Even if we suspected the possibility of vEDS based on the patient's clinical symptoms, the genetic and biomolecular assays could not be easily performed in most hospitals. Fortunately, we obtained advice from an authority in genetics and had technical support with the genetic and biomolecular assays. If this patient had not been definitively diagnosed, it is likely that the patient and his family might have lost any hope. Our belief is that a system for diagnosing rare inherited diseases, such as vEDS, should therefore be established as expeditiously as possible in Japan.

In general, most surgeons encounter vEDS patients who are affected by perforative peritonitis and perform surgery by creating an intestinal stoma, because the abdominal cavity is polluted with stool and the patient's tissues are very fragile. Furthermore, the intestinal stoma helps in the management of constipation, which these patients often experience to a severe extent.¹ The existence of an intestinal stoma is also preferable in order to prevent high intestinal pressures. However, patients who receive a colostomy creation are typically frustrated by the limited lifestyle. Therefore, while we understand why a patient may prefer bowel reconstruction, it is difficult to proceed down this path. It is necessary to consider the future of the vEDS patients, as it may be safer not to remove the intestinal stoma to

prevent high intrabowel pressure that causes constipation and adhesive ileus. It is important to note that complications and tissue weakness increase in vEDS patients after the age of 20 years.^{1,2} Several authors have recommended that the perforative lesion and its distal colon should be removed at the same time to prevent reperforation in the sigmoid colon and rectum.¹⁰ Other authors have also recommended a subtotal colectomy as a reasonable treatment because of the high rate of reperforation in vEDS patients.¹² Although these suggestions have validity and are based on a safety-first concept, we were unable to perform a subtotal colectomy for the present vEDS patient at the time of the first operation, when a definitive diagnosis had not yet been determined. Moreover, it is difficult for us to perform both a partial resection of the small intestine and a subtotal colectomy, even at a second operation, because of the risk of short bowel syndrome and anastomotic leakage. It appears that a unique procedure for perforation of the colon in vEDS patients cannot be standardized, because individual patients have widely divergent background factors, such as age, performance status, accuracy of the diagnosis, frequency of perforation, and medical expertise in their country.

We recommend a therapeutic approach for the ileus in vEDS patients based on the clinical course of the present vEDS patient. vEDS patients who are affected by ileus must be surgically treated before too many fistulas develop in the intestine, regardless of the presence of ischemic changes. In general, patients who are diagnosed with a paralytic ileus or adhesive ileus after prior operations are conservatively treated by decompression with a nasogastric tube or a Miller–Abbott tube. However, we were unable to treat our vEDS patient conservatively, because the wall of his small intestine was easily torn and became necrotic under high pressure. The timing for a surgical operation must be carefully considered, and a massive bowel resection should always be prevented if at all possible.

Acknowledgments. We thank Hiroyuki Naora, MD, PhD, for advising on our results in genetic and biomolecular assays. This study was supported by Research on Intractable Diseases, Ministry of Health, Welfare, and Labor, Japan (#2141039040) (to T.K. and A.H.)

References

1. Pepin M, Schwarze U, Superti-Furga A, Byers PH. Clinical and genetic features of Ehlers–Danlos syndrome type IV, the vascular type. *N Engl J Med* 2000;342:673–80.
2. Watanabe A, Shimada T. The vascular type of Ehlers–Danlos syndrome. *J Nippon Med Sch* 2008;75:254–61.
3. Watanabe A, Kosho T, Wada T, Sakai N, Fujimoto M, Fukushima Y, et al. Genetic aspects of the vascular type of Ehlers–Danlos syndrome (vEDS, EDSIV) in Japan. *Circ J* 2007;71:261–5.
4. Yang JH, Lee ST, Kim JA, Kim SH, Jang SY, Ki CS, et al. Genetic analysis of three Korean patients with clinical features of Ehlers–Danlos syndrome type IV. *J Korean Med Sci* 2007;22:698–705.
5. Hata R, Kurata S, Shinkai H. Existence of malfunctioning pro $\alpha 2(I)$ collagen genes in a patient with a pro $\alpha 2(I)$ -chain-defective variant of Ehlers–Danlos syndrome. *Eur J Biochem* 1988;174:231–7.
6. Hatamochi A, Ono M, Ueki H, Namba M. Regulation of collagen gene expression by transformed human fibroblasts: decreased type I and type III collagen RNA transcription. *J Invest Dermatol* 1991;96:473–7.
7. Fleischmajer R, Perlish JS, Krieg T, Timpl R. Variability in collagen and fibronectin synthesis by scleroderma fibroblasts in primary culture. *J Invest Dermatol* 1981;76:400–3.
8. Okita H, Ikeda Y, Mitsushashi Y, Namikawa H, Kitamura Y, Hama-saki Y, et al. A novel point mutation at donor splice-site in intron 42 of type III collagen gene resulting in the inclusion of 30 nucleotides into the mature mRNA in a case of vascular type of Ehlers–Danlos syndrome. *Arch Dermatol Res* 2009;302:395–9.
9. Matsushima K, Takara H. Endovascular treatment for a spontaneous rupture of the posterior tibial artery in a patient with Ehlers–Danlos syndrome type IV: report of a case. *Surg Today* 2009;39:523–6.
10. Freeman RK, Swegle J, Sise MJ. The surgical complications of Ehlers–Danlos syndrome. *Am Surg* 1996;62:869–73.
11. Privitera A, Milkhu C, Datta V, Sayegh M, Cohen R, Windsor A. Spontaneous rupture of the spleen in type IV Ehlers–Danlos syndrome: report of a case. *Surg Today* 2009;39(1):52–4.
12. Fuchs JR, Fishman SJ. Management of spontaneous colonic perforation in Ehlers–Danlos syndrome type IV. *J Pediatr Surg* 2004;39(2):e1–3.

Mutations affecting components of the SWI/SNF complex cause Coffin-Siris syndrome

Yoshinori Tsurusaki¹, Nobuhiko Okamoto², Hirofumi Ohashi³, Tomoki Kosho⁴, Yoko Imai⁵, Yumiko Hibi-Ko⁵, Tadashi Kaname⁶, Kenji Naritomi⁶, Hiroshi Kawame^{7,8}, Keiko Wakui⁴, Yoshimitsu Fukushima⁴, Tomomi Homma⁹, Mitsuhiro Kato¹⁰, Yoko Hiraki¹¹, Takanori Yamagata¹², Shoji Yano¹³, Seiji Mizuno¹⁴, Satoru Sakazume¹⁵, Takuma Ishii^{15,16}, Toshiro Nagai¹⁵, Masaaki Shiina¹⁷, Kazuhiro Ogata¹⁷, Tohru Ohta¹⁸, Norio Niikawa¹⁸, Satoko Miyatake¹, Ippei Okada¹, Takeshi Mizuguchi¹, Hiroshi Doi¹, Hirotomo Saitsu¹, Noriko Miyake¹ & Naomichi Matsumoto¹

By exome sequencing, we found *de novo* SMARCB1 mutations in two of five individuals with typical Coffin-Siris syndrome (CSS), a rare autosomal dominant anomaly syndrome. As SMARCB1 encodes a subunit of the SWI/SNF complex, we screened 15 other genes encoding subunits of this complex in 23 individuals with CSS. Twenty affected individuals (87%) each had a germline mutation in one of six SWI/SNF subunit genes, including SMARCB1, SMARCA4, SMARCA2, SMARCE1, ARID1A and ARID1B.

Chromatin remodeling factors regulate the gene accessibility and expression by dynamic alteration of chromatin structure. SWI/SNF complexes have important roles in lineage specification, maintenance of stem cell pluripotency and tumorigenesis^{1–5}. These complexes are composed of evolutionarily conserved core subunits and variant subunits. Brahma-associated factor (BAF) and Polybromo BAF (PBAF) complexes constitute two major subclasses^{1–5}. It has been suggested that the BAF complex is similar to the yeast SWI/SNF complex and that the PBAF complex is more like the chromatin remodelling complex (RSC) in yeast, which is required for cell cycle progression through mitosis⁶. However, several subunits that are common

to both BAF and PBAF complexes are predicted to be related to the regulation of lineage- and tissue-specific gene expression².

Coffin-Siris syndrome (MIM 135900) is a rare congenital anomaly syndrome characterized by growth deficiency, intellectual disability, microcephaly, coarse facial features and hypoplastic nail of the fifth finger and/or toe (Fig. 1 and Supplementary Table 1)⁷. The majority of affected individuals represent sporadic cases, which is compatible with an autosomal dominant inheritance mechanism. The genetic cause for this syndrome has not been elucidated.

To identify the genetic basis of CSS, we performed whole-exome sequencing of five typical affected individuals (Supplementary Methods). Taking into account our model that assumes that an abnormality in a causal gene would be shared in two or more subjects, 51 variants were identified as candidates (Supplementary Table 2). All the variants were also examined by Sanger sequencing of PCR products amplified using genomic DNA from the five affected individuals and their parents. Nine variants were found to be false positives, 40 were inherited from either the father or mother, and 2 *de novo* heterozygous mutations of SMARCB1 were found in 2 affected individuals (c.1130G>A (p.Arg377His) and c.1091_1093del AGA (p.Lys364del)) (Table 1, Supplementary Fig. 1 and Supplementary Methods). Two *de novo* coding-sequence mutations occurring within a specific gene is an extremely unlikely event⁸, supporting the idea that SMARCB1 is a causative gene in CSS. Next, we screened SMARCB1 in 23 individuals with CSS by high-resolution melting analysis⁹ and identified the mutation encoding the p.Lys364del alteration in two additional individuals, including one of Arab descent (subject 22) (Table 1 and Supplementary Fig. 1). As the mutation detection rate was relatively low (4 of 23, only 17.4%), we screened 15 additional genes encoding other SWI/SNF subunits (Supplementary Table 3). Unexpectedly, four other subunits, SMARCA4 (also known as BRG1), SMARCE1, ARID1A and ARID1B were also found to be mutated (Table 1 and Supplementary Figs. 2–5). In subject 10, a, c.2144C>T mutation in ARID1B (encoding p.Pro715Leu) was found in addition to the c.5632delG mutation in ARID1B. RT-PCR products that were amplified from total RNA from this subject's lymphoblastoid cells were cloned into the pCR4-TOPO vector. The two mutations were present on different alleles, according to sequencing of clones containing each allele (data not shown). As the c.5632delG mutation is

¹Department of Human Genetics, Yokohama City University Graduate School of Medicine, Yokohama, Japan. ²Division of Medical Genetics, Osaka Medical Center and Research Institute for Maternal and Child Health, Izumi, Japan. ³Division of Medical Genetics, Saitama Children's Medical Center, Iwatsuki, Japan. ⁴Department of Medical Genetics, Shinshu University School of Medicine, Matsumoto, Japan. ⁵Division of Pediatrics, Japanese Red Cross Medical Center, Tokyo, Japan. ⁶Department of Medical Genetics, University of the Ryukyus Faculty of Medicine, Okinawa, Japan. ⁷Department of Genetic Counseling, Graduate School of Humanities and Sciences, Ochanomizu University, Tokyo, Japan. ⁸Division of Medical Genetics, Nagano Children's Hospital, Azumino, Japan. ⁹Division of Pediatrics, Yamagata Prefectural and Sakata Municipal Hospital Organization, Nihonkai General Hospital, Sakata, Japan. ¹⁰Department of Pediatrics, Yamagata University Faculty of Medicine, Yamagata, Japan. ¹¹Hiroshima Municipal Center for Child Health and Development, Hiroshima, Japan. ¹²Department of Pediatrics, Jichi Medical University, Tochigi, Japan. ¹³Genetics Division, Department of Pediatrics, Los Angeles County and University of Southern California Medical Center, Keck School of Medicine, University of Southern California, Los Angeles, California, USA. ¹⁴Department of Pediatrics, Central Hospital, Aichi Human Service Center, Kasugai, Japan. ¹⁵Department of Pediatrics, Koshigaya Hospital, Dokkyo University School of Medicine, Koshigaya, Japan. ¹⁶Nakagawa-No-Sato, Hospital for the Disabled, Saitama, Japan. ¹⁷Department of Biochemistry, Yokohama City University Graduate School of Medicine, Yokohama, Japan. ¹⁸Research Institute of Personalized Health Sciences, Health Sciences University of Hokkaido, Ishikari-Tobetsu, Japan. Correspondence should be addressed to N. Matsumoto (naomat@yokohama-cu.ac.jp) or N. Miyake (nmiyake@yokohama-cu.ac.jp).

Received 29 September 2011; accepted 10 February 2012; published online 18 March 2012; doi:10.1038/ng.2219

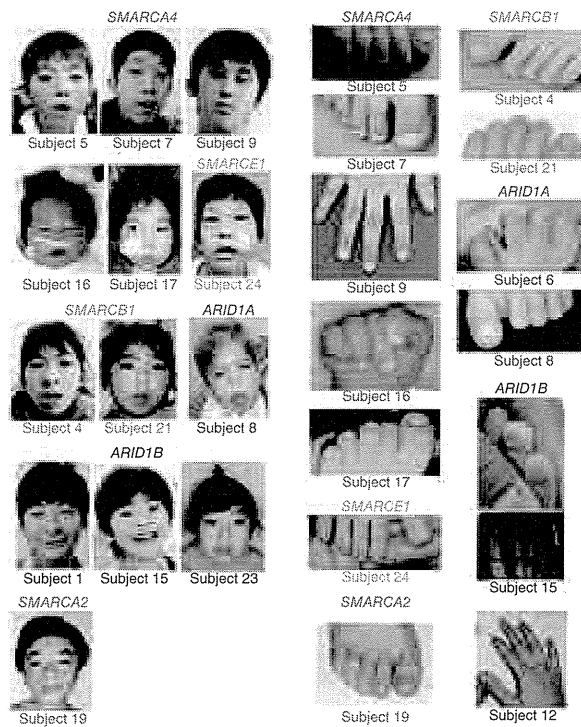


Figure 1 Photographs of individuals with Coffin-Siris syndrome. The faces (left) and hypoplastic-to-absent nail of the fifth finger or toe (right) of affected individuals are shown with the color-coded names of the corresponding mutated genes. The green arrow indicates the absence of the distal phalanx in the fifth toe. No obvious hypoplastic nails were observed in subjects 12 or 19. Consent for all the photographs was obtained from the families of the affected individuals.

in mice¹⁰. However, in humans, abnormalities in both *SMARCA4* and *SMARCA2* are found in CSS, indicating that the in-frame partial deletion of the gene encoding BRM in subject 19 has a specific mutational effect different from that of simple inactivation in mice. These data support the idea that abnormalities in the BRG1-BAF and BRM-BAF complexes can cause the abnormal neurological development in CSS.

All the mutated genes found in CSS, except for *SMARCE1*, have been reported to be associated with tumorigenesis^{1,2}. Among the 23 subjects with CSS, only subject 3 with an *ARID1A* mutation presented with hepatoblastoma. To our knowledge, haploinsufficiency and/or homozygous inactivation of *ARID1A* have been found in several types of cancer but not in hepatoblastoma. Malignancies were not detected in any of the other subjects with CSS examined here. It remains to be seen whether malignancies are robustly associated with CSS.

Given the fact that all the mutations in *ARID1A* and *ARID1B* in CSS were predicted to cause protein truncation, we proposed that haploinsufficiency of these two genes must be able to cause CSS. cDNA analysis of lymphoblastoid cell lines from subjects 1, 6 and 23 indicated that the mutated transcripts were subject to nonsense-mediated mRNA decay (Supplementary Fig. 8). In subject 10, the *ARID1B* mutation associated with the creation of a premature stop codon in the last exon did not result in nonsense-mediated mRNA decay as expected (Supplementary Fig. 8).

In regard to the other mutated genes, germline heterozygous truncation mutations in *SMARCB1* and *SMARCA4* have been reported

very likely to be deleterious (as it results in a truncated protein), the c.2144C>T mutation is likely to be a rare polymorphism. Of note, subject 12, who presented an atypical facial appearance and indistinct hypoplastic nails, had two interstitial deletions at 6q25.3–q27 involving *ARID1B*, as detected by a SNP array (Supplementary Fig. 6 and Supplementary Methods). Furthermore, subject 14 was found to have an interstitial deletion of *SMARCA2* by a SNP array (Supplementary Fig. 7 and Supplementary Methods). No other copy-number changes involving genes encoding SWI/SNF complex components were found in subjects 2, 14 or 18 by array analysis. The overall mutation detection rate was 87%. In total, 20 of the 23 subjects had a mutation affecting one of the six SWI/SNF subunits.

Mutations in CSS were identified in the BAF-specific subunits *ARID1A* and *ARID1B* but not in PBAF-specific subunits (*BRD7*, *ARID2* and *PBRM1*) (Supplementary Table 3). In addition, mutations were identified in *SMARCA4* (*BRG1*) as well as in *SMARCA2* (*BRM*) (Supplementary Table 3). The BRG1 and BRM proteins are mutually exclusive catalytic ATP subunits in mammalian SWI/SNF complexes. Of note, the majority of heterozygous *Smarca4*-null mice survive with susceptibility to neoplasia, with a minority dying after birth because of exencephaly, whereas homozygous *Smarca2*-null mice are viable and fertile⁴. In *Smarca2*-null mice, *Brg1* is upregulated, suggesting that *Brg1* can functionally replace *Brm*

Table 1 Mutations in individuals with Coffin-Siris syndrome

Subject ID	Gene	Mutation	Alteration	Type	Control allele frequency ^a
4	<i>SMARCB1</i>	c.1091_1093del AGA	p.Lys364del	<i>De novo</i>	0/502
11	<i>SMARCB1</i>	c.1130G>A	p.Arg377His	<i>De novo</i>	0/500
21	<i>SMARCB1</i>	c.1091_1093del AGA	p.Lys364del	NC	0/502
22	<i>SMARCB1</i>	c.1091_1093del AGA	p.Lys364del	NC	0/502
9	<i>SMARCA4</i>	c.1636_1638del AAG	p.Lys546del	<i>De novo</i>	0/350
7	<i>SMARCA4</i>	c.2576C>T	p.Thr859Met	<i>De novo</i>	0/368
5	<i>SMARCA4</i>	c.2653C>T	p.Arg885Cys	<i>De novo</i>	0/368
16	<i>SMARCA4</i>	c.2761C>T	p.Leu921Phe	<i>De novo</i>	0/368
25	<i>SMARCA4</i>	c.3032T>C	p.Met1011Thr	NC	0/372
17	<i>SMARCA4</i>	c.3469C>G	p.Arg1157Gly	<i>De novo</i>	0/368
19	<i>SMARCA2</i>	Partial deletion		<i>De novo</i>	–
24	<i>SMARCE1</i>	c.218A>G	p.Tyr73Cys	<i>De novo</i>	0/368
3	<i>ARID1A</i>	c.31_56del	p.Ser11Alafs*91	NC	0/330
6	<i>ARID1A</i>	c.2758C>T	p.Gln920*	NC	0/376
8	<i>ARID1A</i>	c.4003C>T	p.Arg1335*	<i>De novo</i>	–
1	<i>ARID1B</i>	c.1678_1688del	p.Ile560Glyfs*89	<i>De novo</i>	–
15	<i>ARID1B</i>	c.1903C>T	p.Gln635*	<i>De novo</i>	–
23	<i>ARID1B</i>	c.3304C>T	p.Arg1102*	<i>De novo</i>	–
10	<i>ARID1B</i>	c.2144C>T	p.Pro715Leu	NC	0/368
10	<i>ARID1B</i>	c.5632del G	p.Asp1878Metfs*96	NC	0/374
12	<i>ARID1B</i>	Microdeletion		NC	–

NC, not confirmed because parental samples were unavailable.

^aThe numbers indicate the observed allele frequency (alleles harboring the change/total tested alleles) in Japanese controls. None of the mutations was found in dbSNP132, the 1000 Genomes database or the National Heart, Lung, and Blood Institute (NHLBI) GO exome sequencing project database. –, not tested.

BRIEF COMMUNICATIONS

in individuals with rhabdoid tumor predisposition syndromes 1 (RTPS1; MIM 609322) and 2 (RTPS2; MIM 613325)^{11,12}, and various types of *SMARCB1* mutations (missense, in-frame deletion, nonsense and splice site) have been found in the germline of individuals with familial and sporadic schwannomatosis (MIM 162091)^{13,14}. Furthermore, mice with heterozygous knockout of *Smarca4* or *Smarcb1* were prone to tumor development². All the mutations in *SMARCA4* and *SMARCB1* in individuals with CSS were non-truncating (either missense or in-frame deletions), implying that they exert gain-of-function or dominant-negative effects (excluding haploinsufficiency as a cause). It is noteworthy that comparable germline mutations in *SMARCB1* have such different phenotypic consequences in their association with the phenotypes of CSS and schwannomatosis. The *SMARCB1* mutations in CSS and those in schwannomatosis are indeed different according to the Human Gene Mutation Database. With regard to the *SMARCA2* interstitial deletion in CSS, the change maintained the coding sequence reading frame but removed exons 20–27 that encode the HELICc domain. RT-PCR analysis confirmed the deletion of exons 20–27 at the cDNA level (Supplementary Fig. 7). These data suggest the importance of the HELICc domain in the *SMARCA2* protein.

The various types of mutations in the genes encoding different SWI/SNF components resulted in similar CSS phenotypes. This suggests that the SWI/SNF complexes coordinately regulate chromatin structure and gene expression. This is the first report, to our knowledge, of germline mutations in SWI/SNF complex genes associated with a multiple congenital anomaly syndrome, highlighting new biological aspects of SWI/SNF complexes in humans. Similarly, genes encoding SNF2-related proteins, which are implicated as chromatin remodeling factors outside of SWI/SNF complexes, are mutated in different syndromes, including in α -thalassaemia/mental retardation syndrome X-linked (*ATRX*; *ATRX* mutations) and in coloboma, heart defect, atresia choanae, retarded growth and development, genital abnormality and ear abnormality (*CHARGE*) syndrome (*CHD7* haploinsufficiency)³. We expect that more mutations affecting chromatin remodeling factors will be found in different human diseases.

URLs. Human Gene Mutation Database, <https://portal.biobase-international.com/cgi-bin/portal/login.cgi>.

Note: Supplementary information is available on the Nature Genetics website.

ACKNOWLEDGMENTS

We thank all the family members for participating in this study. This work was supported by research grants from the Ministry of Health, Labour and Welfare (to N. Miyake, H.S. and N. Matsumoto), the Japan Science and Technology Agency (to N. Matsumoto), the Strategic Research Program for Brain Sciences (to N. Matsumoto), the Japan Epilepsy Research Foundation (to H.S.) and the Takeda Science Foundation (to N. Matsumoto and N. Miyake). This study was also funded by a Grant-in-Aid for Scientific Research on Innovative Areas (Foundation of Synapse and Neurocircuit Pathology) from the Ministry of Education, Culture, Sports, Science and Technology of Japan (to N. Matsumoto), a Grant-in-Aid for Scientific Research from the Japan Society for the Promotion of Science (to N. Matsumoto), a Grant-in-Aid for Young Scientists from the Japan Society for the Promotion of Science (to N. Miyake and H.S.) and a Grant for 2011 Strategic Research Promotion of Yokohama City University (to N. Matsumoto). This study was performed at the Advanced Medical Research Center at Yokohama City University. Informed consent was obtained from all the families of affected individuals. The Institutional Review Board of Yokohama City University approved this study.

AUTHOR CONTRIBUTIONS

Y.T., S. Miyatake, I.O., H.D., H.S. and N. Miyake performed exome sequencing and Sanger sequencing. Y.T., M.S., K.O., I.O., T.M., H.D., H.S. and N. Miyake performed data management and analysis. N.O., H.O., T. Koshi, Y.I., Y.H.-K., T. Kaname, K.N., H.K., K.W., Y.F., T.H., M.K., Y.H., T.Y., S.Y., S. Mizuno, S.S., T.I., T.N., T.O. and N.N. provided clinical materials after careful evaluation. Y.T., N. Miyake and N. Matsumoto wrote the manuscript. N. Matsumoto designed and oversaw all aspects of the study.

COMPETING FINANCIAL INTERESTS

The authors declare no competing financial interests.

Published online at <http://www.nature.com/naturegenetics/>.

Reprints and permissions information is available online at <http://www.nature.com/reprints/index.html>.

1. Reisman, D., Glaros, S. & Thompson, E.A. *Oncogene* **28**, 1653–1668 (2009).
2. Wilson, B.G. & Roberts, C.W. *Nat. Rev. Cancer* **11**, 481–492 (2011).
3. Clapier, C.R. & Cairns, B.R. *Annu. Rev. Biochem.* **78**, 273–304 (2009).
4. Bultman, S. *et al. Mol. Cell* **6**, 1287–1295 (2000).
5. Hargreaves, D.C. & Crabtree, G.R. *Cell Res.* **21**, 396–420 (2011).
6. Xue, Y. *et al. Proc. Natl. Acad. Sci. USA* **97**, 13015–13020 (2000).
7. Coffin, G.S. & Siris, E. *Am. J. Dis. Child.* **119**, 433–439 (1970).
8. Bamshad, M.J. *et al. Nat. Rev. Genet.* **12**, 745–755 (2011).
9. Wittwer, C.T., Reed, G.H., Gundry, C.N., Vandersteen, J.G. & Pryor, R.J. *Clin. Chem.* **49**, 853–860 (2003).
10. Reyes, J.C. *et al. EMBO J.* **17**, 6979–6991 (1998).
11. Schneppenheim, R. *et al. Am. J. Hum. Genet.* **86**, 279–284 (2010).
12. Taylor, M.D. *et al. Am. J. Hum. Genet.* **66**, 1403–1406 (2000).
13. Boyd, C. *et al. Clin. Genet.* **74**, 358–366 (2008).
14. Hadfield, K.D. *et al. J. Med. Genet.* **45**, 332–339 (2008).





Short Report

Coffin–Siris syndrome is a SWI/SNF complex disorder

Tsurusaki Y, Okamoto N, Ohashi H, Mizuno S, Matsumoto N, Makita Y, Fukuda M, Isidor B, Perrier J, Aggarwal S, Dalal AB, Al-Kindy A, Liebelt J, Mowat D, Nakashima M, Saito H, Miyake N, Matsumoto N. Coffin–Siris syndrome is a SWI/SNF complex disorder. Clin Genet 2013. © John Wiley & Sons A/S. Published by John Wiley & Sons Ltd, 2013

Coffin–Siris syndrome (CSS) is a congenital disorder characterized by intellectual disability, growth deficiency, microcephaly, coarse facial features, and hypoplastic or absent fifth fingernails and/or toenails. We previously reported that five genes are mutated in CSS, all of which encode subunits of the switch/sucrose non-fermenting (SWI/SNF) ATP-dependent chromatin-remodeling complex: *SMARCB1*, *SMARCA4*, *SMARCE1*, *ARID1A*, and *ARID1B*. In this study, we examined 49 newly recruited CSS-suspected patients, and re-examined three patients who did not show any mutations (using high-resolution melting analysis) in the previous study, by whole-exome sequencing or targeted resequencing. We found that *SMARCB1*, *SMARCA4*, or *ARID1B* were mutated in 20 patients. By examining available parental samples, we ascertained that 17 occurred *de novo*. All mutations in *SMARCB1* and *SMARCA4* were non-truncating (missense or in-frame deletion) whereas those in *ARID1B* were all truncating (nonsense or frameshift deletion/insertion) in this study as in our previous study. Our data further support that CSS is a SWI/SNF complex disorder.

Conflict of interest

None of the authors have any conflicts of interest to disclose.

**Y Tsurusaki^a, N Okamoto^b,
H Ohashi^c, S Mizuno^d,
N Matsumoto^e, Y Makita^f,
M Fukuda^g, B Isidor^h, J Perrierⁱ,
S Aggarwal^j, AB Dalal^k,
A Al-Kindy^l, J Liebelt^m,
D Mowatⁿ, M Nakashima^a,
H Saito^a, N Miyake^a
and N Matsumoto^a**

^aDepartment of Human Genetics, Yokohama City University Graduate School of Medicine, Yokohama, Japan, ^bDivision of Medical Genetics, Osaka Medical Center and Research Institute for Maternal and Child Health, Izumi, Japan, ^cDivision of Medical Genetics, Saitama Children's Medical Center, Saitama, Japan, ^dDepartment of Pediatrics, Central Hospital, Aichi Human Service Center, Kasugai, Japan, ^eDepartment of Pediatrics, Asahikawa Medical University, Asahikawa, Japan, ^fEducation Center, Asahikawa Medical University, Asahikawa, Japan, ^gDepartment of Pediatrics, St. Marianna University School of Medicine, Kawasaki, Japan, ^hCHU Nantes, Service de Génétique Médicale, Nantes, France, ⁱCHU Nantes, Service de Pédiatrie, Nantes, France, ^jDepartment of Medical Genetics, Nizam's Institute of Medical Sciences, Hyderabad, India, ^kDiagnostics Division, Centre for DNA Fingerprinting and Diagnostics, Hyderabad, India, ^lDepartment of Genetics, Sultan Qaboos University Hospital, Muscat, Oman, ^mSouth Australian Clinical Genetics Service, SA Pathology at Women's and Children's Hospital, North Adelaide, Australia, and ⁿDepartment of Medical Genetics, Sydney Children's Hospital and the School of Women's and Children's Health, University of New South Wales, Sydney, Australia
Key words: Coffin–Siris syndrome – *ARID1B* – *SMARCA4* – *SMARCB1* – SWI/SNF ATP-dependent chromatin-remodeling complex

Corresponding author: Naomichi Matsumoto MD, PhD, Department of Human Genetics, Yokohama City University Graduate School of Medicine, 3-9 Fukuura, Kanazawa-ku, Yokohama 236-0004, Japan.
Tel.: +81 45 787 2606;
fax: +81 45 786 5219;
e-mail: naomat@yokohama-cu.ac.jp

Received 9 May 2013, revised and accepted for publication 28 June 2013

Coffin–Siris Syndrome (CSS; MIM 135900), first described by Coffin and Siris in 1970, is a congenital disorder characterized by intellectual disability (ID), growth deficiency, microcephaly, coarse facial features, and hypoplastic or absent fifth fingernails and/or toenails (1). Recently, we identified mutations in six genes encoding subunits of the switch/sucrose non-fermenting (SWI/SNF) ATP-dependent chromatin-remodeling complex: *SMARCB1*, *SMARCA4*, *SMARCA2*, *SMARCE1*, *ARID1A*, and *ARID1B* (2). Simultaneously, *SMARCA2* mutations were frequently found in patients with a similar syndrome, Nicolaides–Baraitser syndrome (NCBRS; MIM 601358) (3, 4). In fact, our patient with a *SMARCA2* mutation was clinically re-evaluated and recategorized as NCBRS (personal communication with Professor Raoul CM Hennekam of University of Amsterdam), removing *SMARCA2* as a causative gene for CSS.

Chromatin structure is important for the accessibility of DNA to transcription factors and for gene expression. The SWI/SNF complex modulates chromatin structure and plays important roles in transcription, cell differentiation, DNA repair, and tumor suppression (5, 6). The complexes contain a single ATPase subunit (*SMARCA2* or *SMARCA4*), core subunits consisting of *SMARCB1*, *SMARCC1*, and *SMARCC2*, and form two major subclasses in mammals: BRG1/hBRM-associated factors (BAF) and polybromo-associated BAF (PBAF) complexes. *ARID1A* and *ARID1B* subunits are mutually exclusive and are only present in BAF complexes, whereas *PBRM1*, *ARID2*, and *BRD7* subunits are PBAF-specific (7, 8). In our previous study, we identified CSS-related mutations in the BAF-specific subunits *ARID1A* and *ARID1B* (2).

In this study, we examined 49 newly recruited patients and re-examined three patients who did not show any mutation (by high-resolution melting analysis) in the previous study.

Materials and methods

Subjects and DNA preparation

We collected patients with suspected CSS showing most of core clinical features including ID, growth deficiency, coarse facial features, and hypoplastic/absent fifth fingernails and/or toenails (Fig. 1,

Table 1). NCBRS, a similar condition to CSS (9), is excluded in this study. Genomic DNA of peripheral blood leukocytes was extracted by conventional methods. Detailed clinical information was obtained after written informed consent was secured from the family members (Table 1). The institutional review board of Yokohama City University School of Medicine approved this study.

Whole-exome sequencing and targeted resequencing

We performed whole-exome sequencing (WES) for 44 patients as previously described (10) and targeted resequencing in eight patients using a HaloPlex Target Enrichment System (Agilent Technologies, Santa Clara, CA) according to the manufacturer's protocol. A probe library was designed with oligonucleotide probes targeting 21 genes encoding SWI/SNF complex subunits (*ACTB*, *ACTL6A*, *ACTL6B*, *ARID1A*, *ARID1B*, *ARID2*, *BRD7*, *DPF1*, *DPF2*, *DPF3*, *PBRM1*, *PHF10*, *SMARCA2*, *SMARCA4*, *SMARCB1*, *SMARCC1*, *SMARCC2*, *SMARCD1*, *SMARCD2*, *SMARCD3*, and *SMARCE1*).

Priority scheme

Out of all variants within exons or ± 2 bp from the exon–intron boundaries, those registered in dbSNP135, the 1000 Genomes Project, and the National Heart Lung and Blood Institute Exome Sequencing Project Exome Variant Server (NHLBI-ESP 5400), our in-house databases (408 exomes) or located within segmental duplications were removed.

Sanger sequencing

Variants were confirmed as true positives by Sanger sequencing on an ABI3500xl or ABI3130xl autosequencer (Life Technologies, Carlsbad, CA). Sequencing data were analyzed with Sequencher software (Gene Codes Corporation, Ann Arbor, MI). Parental samples were also confirmed (when available) to check the inheritance of variants.

Results

By WES, the mean coverage of RefSeq coding sequence was 49.6–175.6 reads, with 72.0–93.2%

Coffin–Siris syndrome is a SWI/SNF complex disorder

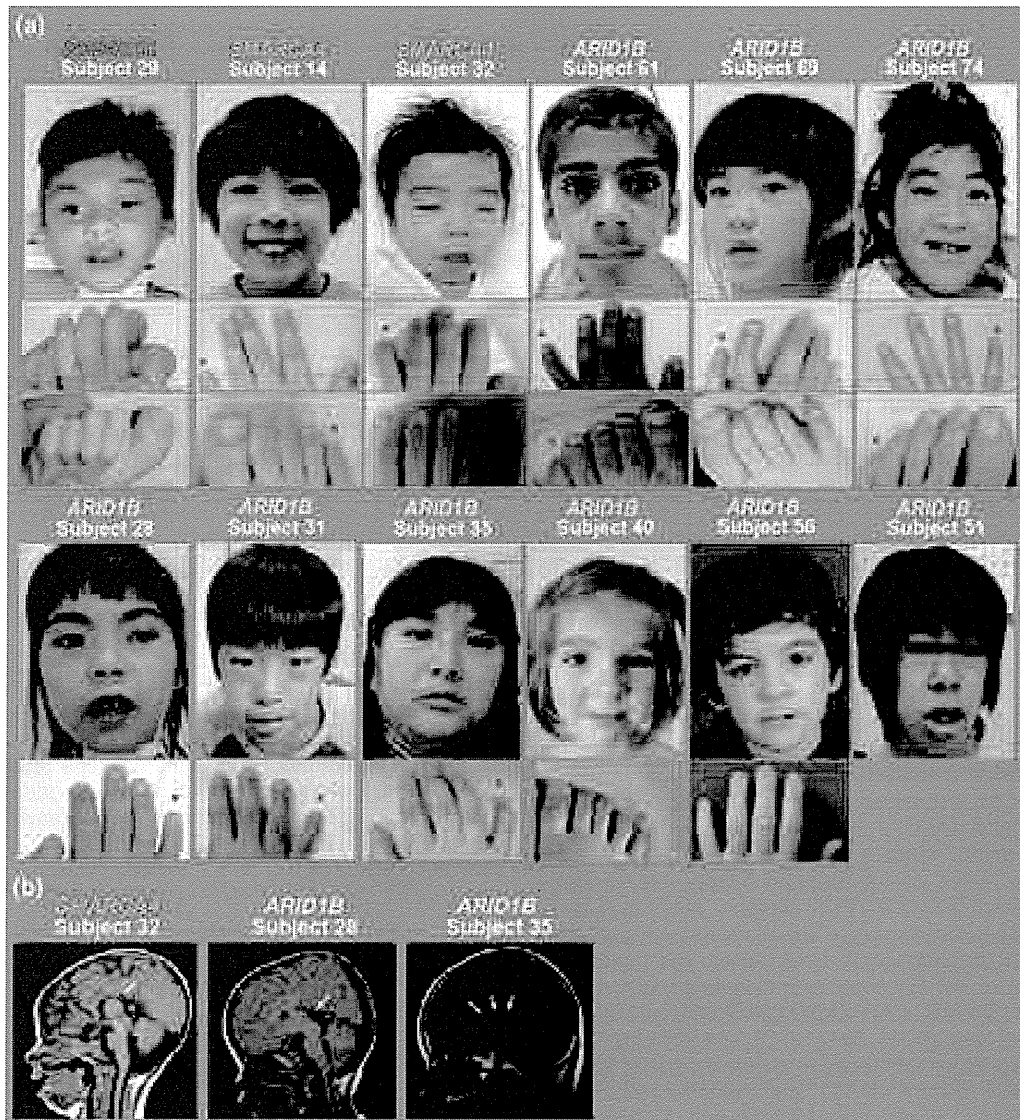


Fig. 1. Photographs and brain magnetic resonance imaging findings in patients with Coffin–Siris syndrome. (a) Faces (top) and nails of the fingers (middle) or/and toes (bottom) of patients, with the mutated gene indicated. Red asterisks indicate the fifth finger/toe. (b) T1-weighted midline sagittal magnetic resonance images. The individuals showed agenesis of the corpus callosum (arrows).

being covered by 20 or more reads. By targeted resequencing, the mean coverage of coding sequence in the target genes was 496.1–541.0 reads, with 96.5–97.2% being covered by 20 or more reads.

Mutations were discovered in *SMARCB1* (3 of 52 patients, 5.8%), *SMARCA4* (2 of 52 patients, 3.8%), and *ARID1B* (15 of 52 patients, 28.8%); all were confirmed by Sanger sequencing. We ascertained that a total of 17 mutations (among 20 patients) occurred *de novo*. No other pathological variants were found. In our previous study, mutations were found in *SMARCB1* (4 of 22 patients, 18.2%), *SMARCA4* (6 of 22 patients, 27.3%),

ARID1B (5 of 22 patients, 22.7%), *ARID1A* (3 of 22 patients, 13.6%), and *SMARCE1* (1 of 22 patients, 4.5%). In this and our previous study, mutations in *SMARCB1* and *SMARCA4* were all non-truncating, implying that they exert gain-of-function or dominant negative effects whereas those in *ARID1B* mutations were all truncating, leading to haploinsufficiency (2). In total, 39 out of 71 CSS patients (54.9%) carry a mutation in one of five genes encoding a SWI/SNF complex subunit (Table 2; Figs S1 and S2). All the mutations are mutually exclusive.

Table 1. Clinical features in CSS

Clinical features	Mutated gene											Mutation positive All	Mutation negative	Fischer's exact two-sided test <i>P</i> values ^a	
	Tsurusaki et al. (2)					This study			Total						
	1B	B1	A4	1A	E1	1B	B1	A4	1B	B1	A4				
Neurodevelopment															
Developmental delay	5/5	4/4	6/6	3/3	1/1	15/15	1/1	2/2	20/20	5/5	8/8	37/37	8/8	1.000	
Hypotonia	4/5	4/4	4/6	2/3	1/1	14/15	0/1	1/2	18/20	4/5	5/8	30/37	7/8	1.000	
Microcephaly	1/5	2/3	4/5	1/3	1/1	2/15	1/1	0/2	3/20	3/4	4/7	12/35	3/8	1.000	
Small cerebellum	0/5	2/3	0/3	1/2		1/15	0/1	1/2	1/20	2/4	1/5	5/31	0/6	0.567	
Seizures	2/5	2/4	2/6	0/2		5/15	1/1	0/2	7/20	3/5	2/8	12/35	4/8	0.443	
Dandy-Walker	0/5	0/2	1/5	1/3		1/14	0/1	1/2	1/19	0/3	2/7	4/32	0/7	1.000	
Abnormal corpus callosum	1/2	2/2	1/1	3/3		6/13	0/1	1/2	7/15	2/3	2/3	14/24	2/6	0.378	
Vision problem	1/4	2/3	5/6	1/2		2/15	0/1	0/2	3/19	2/4	5/8	11/33	3/7	0.679	
Hearing loss	1/5	3/4	3/6	1/2	1/1	1/15	1/1	1/2	2/20	4/5	4/8	12/36	0/7	0.163	
Ectodermal															
Absent/hypoplastic fifth finger/toenails	5/5	4/4	6/6	3/3	1/1	11/15	1/1	2/2	16/20	5/5	8/8	33/37	4/7	0.068	
Hirsutism	5/5	3/4	6/6	3/3	1/1	14/15	1/1	2/2	19/20	4/5	8/8	35/37	7/7	1.000	
Sparse scalp hair	3/5	4/4	3/6	3/3	1/1	7/15	1/1	1/2	10/20	5/5	4/8	23/37	1/7	0.035	
Thick eyebrow	5/5	4/4	6/6	2/3	1/1	15/15	1/1	2/2	20/20	5/5	8/8	36/37	8/8	1.000	
Long eyelashes	4/5	4/4	6/6	3/3	1/1	13/15	1/1	2/2	17/20	5/5	8/8	34/37	7/8	0.557	
Abnormal/delayed dentition	5/5	3/3	3/5	2/2	1/1	4/10	1/1	0/1	9/15	4/4	3/6	19/28	0/6	0.004	
Non-functioning/absent tear duct	0/1	2/3	1/4	0/2	0/1	2/14	0/1	0/2	2/15	2/4	1/6	5/28	0/7	0.559	
Facial															
Coarse appearance	5/5	4/4	6/6	3/3	1/1	15/15	1/1	2/2	20/20	5/5	8/8	37/37	8/8	1.000	
Flat nasal bridge	5/5	3/4	4/6	2/3	1/1	12/15	1/1	2/2	17/20	4/5	6/8	30/37	6/8	0.652	
Broad nose	5/5	4/4	2/6	2/3	1/1	13/15	1/1	2/2	18/20	5/5	4/8	30/37	6/8	0.652	
Wide mouth	3/5	4/4	3/6	3/3	1/1	13/15	1/1	2/2	16/20	5/5	5/8	30/37	6/8	0.652	
Thick lips	5/5	4/4	5/6	3/3	1/1	15/15	1/1	2/2	20/20	5/5	7/8	36/37	8/8	1.000	
Abnormal ears	4/5	4/4	5/6	3/3	1/1	9/15	1/1	2/2	13/20	5/5	7/8	29/37	1/7	0.002	
High palate	5/5	4/4	5/5	2/3	1/1	9/15	1/1	2/2	14/20	5/5	7/7	29/36	6/8	0.659	
Cleft palate	0/5	2/4	3/6	2/3	1/1	1/15	0/1	1/2	1/20	2/5	4/8	10/37	0/8	0.169	
Ptosis	0/5	3/4	5/6	0/3	1/1	3/15	0/1	1/2	3/20	3/5	6/8	13/37	3/8	1.000	
Macroglossia	0/5	3/4	2/6	0/3	1/1	2/15	0/1	0/2	2/20	3/5	2/8	8/37	0/7	0.318	
Short philtrum	0/5	0/4	3/6	1/3	1/1	6/15	1/1	1/2	6/20	1/5	4/8	13/37	1/8	0.402	
Long philtrum	1/5	2/4	0/6	1/3	0/1	5/12	0/1	0/1	6/17	2/5	0/7	9/33	1/8	0.653	
Skeletal															
Absent/hypoplastic fifth phalanx (hand)	5/5	1/1	4/5	2/2	1/1	5/14		2/2	10/19	1/1	6/7	20/30	2/8	0.050	
Absent/hypoplastic fifth phalanx (foot)	4/5	1/1	3/3	2/2	1/1	7/12		2/2	11/17	1/1	5/5	20/26	3/7	0.161	
Short stature	2/5	4/4	4/5	2/3	1/1	10/14	1/1	1/2	12/19	5/5	5/7	25/35	6/8	1.000	
Spinal anomalies	3/4	3/4	1/4	1/2	1/1	3/14	1/1	0/2	6/18	4/5	1/6	13/32	3/7	1.000	
Delayed bone age	0/1	1/1		1/2		2/11		0/1	2/12	1/1	0/1	4/16	4/6	0.137	

Table 1. Continued.

Clinical features	Mutated gene										Mutation positive	Fischer's exact two-sided test <i>P</i> values ^a	
	Tsurusaki et al. (2)					This study							Total
	1B	B1	A4	1A	E1	1B	B1	A4	1B	B1			
Gastrointestinal	4/5	3/4	4/6	3/3	1/1	10/15	1/1	2/2	14/20	5/5	7/8	30/37	1.000
Feeding problems	4/5	2/4	2/6	1/3	1/1	11/15	1/1	2/2	15/20	5/5	7/8	30/36	0.623
Sucking problems	1/5	1/4	2/5	2/2	0/1	1/15	0/1	0/2	2/20	1/5	2/7	7/34	1.000
Intestinal anomalies	0/5	0/4	0/6	1/3	0/1	0/15	0/1	0/2	0/20	0/5	0/8	1/37	1.000
Tumor	5/5	3/4	4/6	3/3	1/1	6/15	1/1	1/2	11/20	4/5	5/8	24/37	0.692
Others	1/5	2/4	2/6	1/3	1/1	6/15	1/1	2/2	7/20	3/5	4/8	16/37	1.000
Frequent infections	2/4	2/3	2/6	2/3	1/1	7/15	1/1	1/2	9/19	3/4	3/8	18/35	1.000
IUGR	1/5	2/4	2/6	3/3	1/1	3/15	0/1	0/2	4/20	2/5	2/8	12/37	1.000
Joint laxity	1/4	1/2	1/6	1/2	0/1	1/15	1/1	0/2	2/19	2/3	1/8	6/83	0.570
Cardiac findings	0/5	2/4	2/6	1/3	0/1	0/15	1/1	1/2	0/20	3/5	3/8	7/37	1.000
Genital findings	0/4	0/4	1/6	0/3	0/1	0/15	1/1	1/2	0/19	1/5	2/8	3/36	0.566
Inguinal hernia	0/4	0/3	0/4	0/2	0/1	2/15	0/1	0/2	2/17	1/4	0/6	3/80	1.000
Umbilical hernia	0/4	0/3	0/4	0/3	0/1	0/15	0/1	0/2	0/20	1/5	0/7	1/36	1.000
Renal findings	0/5	1/4	0/5	0/3	0/1	0/15	0/1	0/2	0/20	1/5	0/7	1/36	1.000
Diaphragmatic hernia													

CSS, Coffin–Siris syndrome; 1B, *ARID1B*; B1, *SMARCB1*; A4, *SMARCA4*; 1A, *ARID1A*; E1, *SMARCE1*; IUGR, Intrauterine growth restriction
^a*P* values for deviation from expected distribution of mutation-positive and mutation-negative subjects.

Discussion

On the basis of this and our previous mutation survey, the mutation detection rates in CSS are 54.9% (39 out of 71) and *ARID1B* mutations are the most common genetic cause of CSS (20 of 71 patients, 28.2%). Santen et al. also found truncating mutations of *ARID1B* in three CSS patients by WES (11). All *ARID1B* mutations reported in CSS are truncating (Figs S1 and S2). Interestingly, Hoyer et al. also reported that *ARID1B* truncating mutations are a frequent cause of unspecific moderate-severe ID (12) (Fig. S1). All of the mutations found in ID were truncating. Some ID patients showed characteristic coarse facial features similar to CSS. Furthermore, hypoplastic/absent fifth finger/toe nails have been described in some ID patients (12). Therefore, taking into consideration the symptoms of CSS, some of the ID patients may also have CSS or these patients and CSS patients are phenotypically overlapped.

We tried to find characteristic clinical features of CSS specific to particular mutated genes. It is only noted that all the CSS patients with *SMARCB1*, *SMARCA4*, *ARID1A* or *SMARCE1* mutations showed hypoplastic/absent fifth finger/toe nails, but some patients with *ARID1B* mutations did not. Except for that, it is difficult to clinically differentiate patients by mutant genes partly due to variable phenotypes in CSS. These findings may suggest that different subunits of the SWI/SNF complex coordinately regulate chromatin and gene expression as a functional unit (13).

Clinical features were compared between patients with identified mutations of genes encoding a SWI/SNF complex subunit and patients without identified SWI/SNF complex subunit mutations using Fisher's exact test (Table 1). Four clinical features showed significant difference including sparse scalp hair (*P* = 0.035), abnormal/delayed dentition (*P* = 0.004), abnormal ears (*P* = 0.002), and absent/hypoplastic fifth phalanx of the hand (*P* = 0.050), although the number of mutation-negative patients is small.

The SWI/SNF complex plays an important role in tumor suppression (7). Mutations in *SMARCB1* were first reported in human cancer (14, 15). Most mutations in *SMARCB1* were truncating mutations and were mainly found in malignant rhabdoid tumors (MRTs) somatically and in the germ line. Furthermore, germ line mutations in *SMARCB1* were also found in schwannomatosis. The *SMARCB1* mutations arise somatically or in the germ line, the second allele was also altered by copy neutral loss of heterozygosity (LOH) as a second hit in the tumor cells. In addition, one family with MRTs was reported as having a germ line nonsense mutation in *SMARCA4* (14, 16). This nonsense mutation is not found in mRNA of immortalized B cells, indicating nonsense-mediated mRNA decay as the molecular mechanism for the lack of *SMARCA4* expression together with copy neutral LOH encompassing *SMARCA4* as a second hit in the tumor cells. To date, these patients having tumors with germline mutations in *SMARCB1* or *SMARCA4*

Y. Tsurusaki et al.

Table 2. Mutations found in patients with Coffin–Siris syndrome

Patient ID	Gene	RefSeq accession number	Nucleotide change	Amino acid change	Mutation	Type	Reference
4	<i>SMARCB1</i>	NM_003073.3	c.1091_1093del	p.Lys364del	Inframeshift	<i>de novo</i>	Tsurusaki et al. (2)
21	<i>SMARCB1</i>	NM_003073.3	c.1091_1093del	p.Lys364del	Inframeshift	nc	Tsurusaki et al. (2)
22	<i>SMARCB1</i>	NM_003073.3	c.1091_1093del	p.Lys364del	Inframeshift	nc	Tsurusaki et al. (2)
29	<i>SMARCB1</i>	NM_003073.3	c.1091_1093del	p.Lys364del	Inframeshift	<i>de novo</i>	This report
37	<i>SMARCB1</i>	NM_003073.3	c.1091_1093del	p.Lys364del	Inframeshift	<i>de novo</i>	This report
48	<i>SMARCB1</i>	NM_003073.3	c.1091_1093del	p.Lys364del	Inframeshift	<i>de novo</i>	This report
11	<i>SMARCB1</i>	NM_003073.3	c.1130G>A	p.Arg377His	Missense	<i>de novo</i>	Tsurusaki et al. (2)
32	<i>SMARCA4</i>	NM_001128849.1	c.1372_1395del	p.Lys458_Glu465del	Inframeshift	<i>de novo</i>	This report
9	<i>SMARCA4</i>	NM_001128849.1	c.1636_1638del	p.Lys546del	Inframeshift	<i>de novo</i>	Tsurusaki et al. (2)
7	<i>SMARCA4</i>	NM_001128849.1	c.2576C>T	p.Thr859Met	Missense	<i>de novo</i>	Tsurusaki et al. (2)
5	<i>SMARCA4</i>	NM_001128849.1	c.2653C>T	p.Arg885Cys	Missense	<i>de novo</i>	Tsurusaki et al. (2)
14	<i>SMARCA4</i>	NM_001128849.1	c.2654G>A	p.Arg885His	Missense	<i>de novo</i>	This report
16	<i>SMARCA4</i>	NM_001128849.1	c.2761C>T	p.Leu921Phe	Missense	<i>de novo</i>	Tsurusaki et al. (2)
25	<i>SMARCA4</i>	NM_001128849.1	c.3032T>C	p.Met1011Thr	Missense	<i>de novo</i>	Tsurusaki et al. (2)
17	<i>SMARCA4</i>	NM_001128849.1	c.3469C>G	p.Arg1157Gly	Missense	<i>de novo</i>	Tsurusaki et al. (2)
38	<i>ARID1B</i>	NM_020732.3	c.1389_1398del	p.Ala464Serfs*35	Frameshift	<i>de novo</i>	This report
28	<i>ARID1B</i>	NM_020732.3	c.1392_1402del	p.Gln467Argfs*64	Frameshift	<i>de novo</i>	This report
1	<i>ARID1B</i>	NM_020732.3	c.1678_1688del	p.Ile560Glyfs*89	Frameshift	<i>de novo</i>	Tsurusaki et al. (2)
40	<i>ARID1B</i>	NM_020732.3	c.1713del	p.Gly572Glufs*21	Frameshift	<i>de novo</i>	This report
15	<i>ARID1B</i>	NM_020732.3	c.1903C>T	p.Gln635*	Nonsense	<i>de novo</i>	Tsurusaki et al. (2)
61	<i>ARID1B</i>	NM_020732.3	c.2062del	p.Leu688Serfs*9	Frameshift	<i>de novo</i>	This report
75	<i>ARID1B</i>	NM_020732.3	c.2891_2892insAC	p.Phe964Leufs*5	Frameshift	<i>de novo</i>	This report
23	<i>ARID1B</i>	NM_020732.3	c.3304C>T	p.Arg1102*	Nonsense	<i>de novo</i>	Tsurusaki et al. (2)
53	<i>ARID1B</i>	NM_020732.3	c.3481G>T	p.Glu1161*	Nonsense	<i>de novo</i>	This report
74	<i>ARID1B</i>	NM_020732.3	c.4009C<T	p.Arg1337*	Nonsense	nc	This report
56	<i>ARID1B</i>	NM_020732.3	c.4820_4825delinsAGGCT	p.Thr1607Lysfs*7	Frameshift	<i>de novo</i>	This report
69	<i>ARID1B</i>	NM_020732.3	c.4821del	p.Pro1609Leufs*5	Frameshift	<i>de novo</i>	This report
27	<i>ARID1B</i>	NM_020732.3	c.4911G>A	p.Trp1637*	Nonsense	<i>de novo</i>	This report
34	<i>ARID1B</i>	NM_020732.3	c.4916_4917del	p.Val1639Aspfs*5	Frameshift	<i>de novo</i>	This report
35	<i>ARID1B</i>	NM_020732.3	c.5623_5625delinsTGACGTCT	p.Ala1875*	Nonsense	nc	This report
10	<i>ARID1B</i>	NM_020732.3	c.5632del	p.Asp1878Metfs*96	Frameshift	nc	Tsurusaki et al. (2)
51	<i>ARID1B</i>	NM_020732.3	c.6120C>G	p.Tyr2040*	Nonsense	nc	This report
31	<i>ARID1B</i>	NM_020732.3	c.6382C>T	p.Arg2128*	Nonsense	<i>de novo</i>	This report
55	<i>ARID1B</i>	NM_020732.3	c.6516C>G	p.Tyr2172*	Nonsense	<i>de novo</i>	This report
12	<i>ARID1B</i>	NM_020732.3			Microdeletion	nc	Tsurusaki et al. (2)
3	<i>ARID1A</i>	NM_006015.4	c.31_56del	p.Ser11Alafs*91	Frameshift	nc	Tsurusaki et al. (2)
6	<i>ARID1A</i>	NM_006015.4	c.2758C>T	p.Gln920*	Nonsense	nc	Tsurusaki et al. (2)
8	<i>ARID1A</i>	NM_006015.4	c.4003C>T	p.Arg1335*	Nonsense	<i>de novo</i>	Tsurusaki et al. (2)
24	<i>SMARCE1</i>	NM_003079.4	c.218A>G	p.Tyr73Cys	Missense	<i>de novo</i>	Tsurusaki et al. (2)

nc, not confirmed, as parental samples were unavailable.

have not been reported in association with the CSS phenotype. It is still unclear why germ line mutations in the same genes can give rise to CSS or different types of tumors. Heterozygous knockout mice were born and appeared normal, but these mice started developing tumors (14). In human, *SMARCB1* and *SMARCA4* mutations in CSS patients were all missense mutations or in-frame deletion while the majority of patients with tumors showed truncating mutations. These evidences might indicate that mutations in CSS were a gain-of-function or a dominant-negative type while those in patients with tumors resulted in the loss of function. Tumor formation was only found in one of our CSS patients carrying an *ARID1A* mutation, who presented with hepatoblastoma and carried an *ARID1A* mutation (2) (Table 1). Mutations in *ARID1A* are undoubtedly involved in the formation of various tumors, but unfortunately autopsy was not performed in the CSS patient and the tumor tissue was unavailable.

Furthermore, germline mutations of *ARID1A* have been unreported in relation to patients with tumors so far. Careful follow-ups should be undertaken to monitor potential tumor development in these CSS patients.

In conclusion, we identified mutations in *SMARCB1*, *SMARCA4*, and *ARID1B* in 20 out of 52 CSS-suspected patients using WES or targeted resequencing. Further investigation of more patients is necessary to validate phenotype–genotype correlations and tumor susceptibility. In yeast, function of SWI/SNF complex is well characterized. SWI/SNF complexes interact with some transcription factors and regulate the expression of hundreds of genes (6), suggesting that other upstream or downstream genes may be mutated in CSS. Further research is needed to understand the pathomechanism of CSS.

Coffin–Siris syndrome is a SWI/SNF complex disorder

Supporting Information

The following Supporting information is available for this article:

Fig.S1 Protein structure of SMARCB1, SMARCA4, and ARID1B with functional domains. Mutations identified in this study are indicated above the structure, and those identified in the previous study and other studies corresponding to Coffin–Siris syndrome or ID (11, 12) are indicated below the structure. SMARCB1 contains two sucrose non-fermenting 5 (SNF5) domains. SMARCA4 contains a conserved Gln, Leu, Gln (QLQ) motif, a helicase/SANT-associated (HSA) domain, a Brahma and Kismet (BRK) domain, DEAD-like helicases superfamily (DEXDc) and helicase superfamily c-terminal (HELICc) domains, and a bromodomain (BROMO). ARID1B contains an ARID/BRIGHT DNA-binding (ARID) domain.

Fig.S2 Number of Coffin–Siris syndrome patients with a mutation in each SWI/SNF complex subunit gene.

Additional Supporting information may be found in the online version of this article.

Acknowledgments

We thank the patients and their families for participating in this work. We also thank Ms. N. Watanabe for technical assistance. This work was supported by Ministry of Health, Labour, and Welfare (H. S., N. Miyake and N. Matsumoto), the Japan Science and Technology Agency (N. Matsumoto), the Strategic Research Program for Brain Sciences (N. Matsumoto) and a Grant-in-aid for Scientific Research on Innovative Areas-(Transcription cycle)-from the Ministry of Education, Culture, Sports, Science, and Technology of Japan (N. Miyake and N. Matsumoto), a Grant-in-aid for Scientific Research from the Japan Society for the Promotion of Science (N. Matsumoto), a Grant-in-aid for Young Scientists from the Japan Society for the Promotion of Science (H. S., N. Miyake and N. Matsumoto), and a grant from the Takeda Science Foundation (N. Miyake and N. Matsumoto).

References

1. Coffin GS, Siris E. Mental retardation with absent fifth fingernail and terminal phalanx. *Am J Dis Child* 1970; 119: 433–439.
2. Tsurusaki Y, Okamoto N, Ohashi H et al. Mutations affecting components of the SWI/SNF complex cause Coffin–Siris syndrome. *Nat Genet* 2012; 44: 376–378.
3. Van Houdt JK, Nowakowska BA, Sousa SB et al. Heterozygous missense mutations in SMARCA2 cause Nicolaides-Baraitser syndrome. *Nat Genet* 2012; 44: 445–449.
4. Wolff D, Ende S, Azzarello-Burri S et al. In-frame deletion and missense mutations of the C-terminal helicase domain of SMARCA2 in three patients with Nicolaides–Baraitser syndrome. *Mol Syndromol* 2012; 2: 237–244.
5. Amankwah EK, Thompson RC, Nabors LB et al. SWI/SNF gene variants and glioma risk and outcome. *Cancer Epidemiol* 2013; 37: 162–165.
6. Santen GW, Kriek M, van Attikum H. SWI/SNF complex in disorder: SWItching from malignancies to intellectual disability. *Epigenetics* 2012a; 7: 1219–1224.
7. Wilson BG, Roberts CW. SWI/SNF nucleosome remodellers and cancer. *Nat Rev Cancer* 2011; 11: 481–492.
8. Euskirchen G, Auerbach RK, Snyder M. SWI/SNF chromatin-remodeling factors: multiscale analyses and diverse functions. *J Biol Chem* 2012; 287: 30897–30905.
9. Castori M, Covaciu C, Rinaldi R et al. A rare cause of syndromic hypotrichosis: Nicolaides–Baraitser syndrome. *J Am Acad Dermatol* 2008; 59: S92–98.
10. Saitsu H, Nishimura T, Muramatsu K et al. De novo mutations in the autophagy gene WDR45 cause static encephalopathy of childhood with neurodegeneration in adulthood. *Nat Genet* 2013; 45: 445–449.
11. Santen GW, Aten E, Sun Y et al. Mutations in SWI/SNF chromatin remodeling complex gene ARID1B cause Coffin–Siris syndrome. *Nat Genet* 2012b; 44: 379–380.
12. Hoyer J, Ekici AB, Ende S et al. Haploinsufficiency of ARID1B, a member of the SWI/SNF-a chromatin-remodeling complex, is a frequent cause of intellectual disability. *Am J Hum Genet* 2012; 90: 565–572.
13. Ronan JL, Wu W, Crabtree GR. From neural development to cognition: unexpected roles for chromatin. *Nat Rev Genet* 2013; 14: 347–359.
14. Romero OA, Sanchez-Cespedes M. The SWI/SNF genetic blockade: effects in cell differentiation, cancer and developmental diseases. *Oncogene* 2013; Epub ahead of print.
15. Versteeg I, Sevenet N, Lange J et al. Truncating mutations of hSNF5/INI1 in aggressive paediatric cancer. *Nature* 1998; 394: 203–206.
16. Schneppenheim R, Fruhwald MC, Gesk S et al. Germline nonsense mutation and somatic inactivation of SMARCA4/BRG1 in a family with rhabdoid tumor predisposition syndrome. *Am J Hum Genet* 2010; 86: 279–284.